INTRINSIC AND SYNAPTIC PROPERTIES OF MEMBRANE CHANNELS IN

MEDIATING THALAMOCORTICAL NETWORK NEURONAL ACTIVITIES: A

COMPUTATIONAL ANALYSIS

AN ABSTRACT

SUBMITTED ON THE 5TH DAY OF MAY 2021

TO THE PROGRAM OF NEUROSCIENCE

IN PARTIAL FULLFILLMENT OF THE REQUIREMENTS

OF THE SCHOOL OF SCIENCE AND ENGINEERING

OF TULANE UNIVERSITY

FOR THE DEGREE

OF

MASTER OF SCIENCE

BY

_____

Hanyun Wang

APPROVED: _____
Laura A. Schrader, Ph.D.

_____
Carmen C. Canavier, Ph.D.

_____
Jeffrey G. Tasker, Ph.D.

Abstract

The thalamocortical network generates rhythmic oscillations of various frequencies that underlie different brain states. Importantly, the transition from a faster frequency of firing, spindle, to slower oscillations, spike and wave discharges, is indicative of the pathological epileptic seizure development. Previous investigations have shown that the complex interactions between neurons in the thalamocortical network based on intrinsic and synaptic properties give rise to the observed frequency changes. However, the exact mechanism of how perturbations in this circuit disrupt the oscillations is not known. In this project, we used a well-established thalamocortical network computational model to perform receptor conductance changes to see how the oscillatory activity in the thalamocortical network changes. Computational methods can be used to provide some mathematical explanations regarding the mechanism of oscillations. Therefore, we generated several phase resetting curves by perturbing neurons during its oscillating period. Our results showed that the frequency reduction under the pathological state in the thalamocortical network might be caused by hyper-synchronization of neuronal activities in this circuit mediated by glutamatergic AMPA receptors. Notably, thalamic reticular neurons are capable of firing at a faster or slower frequency depending on the timing of the input that they receive from other neurons. Overall, our results provided evidence to support the hypothesis that thalamic reticular neurons might be the ultimate pacemakers in the thalamocortical network.

INTRINSIC AND SYNAPTIC PROPERTIES OF MEMBRANE CHANNELS IN

MEDIATING THALAMOCORTICAL NETWORK NEURONAL ACTIVITIES: A

COMPUTATIONAL ANALYSIS

A THESIS

SUBMITTED ON THE 5TH DAY OF MAY 2021

TO THE PROGRAM OF NEUROSCIENCE

IN PARTIAL FULLFILLMENT OF THE REQUIREMENTS

OF THE SCHOOL OF SCIENCE AND ENGINEERING

OF TULANE UNIVERSITY

FOR THE DEGREE

OF

MASTER OF SCIENCE

BY

_____

Hanyun Wang

APPROVED: _____

Laura A. Schrader, Ph.D.

_____

Carmen C. Canavier, Ph.D.

_____
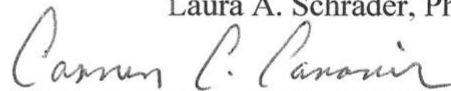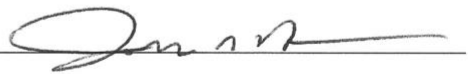
Jeffrey G. Tasker, Ph.D.

Acknowledgments

I would like to thank my advisor, Dr. Laura Schrader, for investing hours of time brainstorming ideas and editing drafts of this thesis.

I would also like to thank Dr. Carmen Canavier, who guided me on modeling network of activities and shared her expertise on phase resetting theory and helped me to come up with hypotheses and to find tools to test the hypotheses for this thesis project. She also shared critical comments to improve this thesis.

Christopher Knowlton, who is a postdoctoral researcher at Dr. Canavier's lab at the time of writing this thesis, generously helped me on writing codes for generating phase response curves for this thesis project.

The bulk of this thesis project is an extension of the work on the Shox2 project where Isabella Febbo, who is a 5th year PhD student at Dr. Schrader's lab at the time of writing this thesis, contributed a lot to. She also offered generous help on trouble-shooting the NEURON program.

Additionally, I would also like to thank Dr. Jeffrey Tasker for being on my committee and offered valuable insights on the results of this thesis project.

TABLE OF CONTENTS

Chapter

Appendix

LIST OF TABLES

LIST OF FIGURES

Introduction

Rhythmic oscillations of brain activity measured by electroencephalograms (EEGs) are thought to underlie various brain states, and the thalamocortical network generates oscillations of various frequencies that can occur both during sleep and wake cycles (Thierry Bal & McCormick, 1996; Steriade et al., 1993). Sleep is distinguished by several oscillations, including slow waves and spindles (Steriade et al., 1993; Steriade & Amzica, 1998). Sleep spindles are characterized by waxing and waning oscillations with a frequency between 10 and 16 Hz and duration between 0.5 and 2 s (Jankel & Niedermeyer, 1985) and are a hallmark of non-rapid eye movement (NREM) sleep stage N2. Interestingly, clinical observations demonstrate an interaction between sleep and seizures (Byars et al., 2008; Kotagal & Yardi, 2008). Spike-and-wave discharges (SWDs), an EEG signature of absence seizures, occur during NREM sleep and can generate from sleep spindles. A similar transition from sleep spindles to SWDs has been demonstrated in an animal model of intramuscular injection of penicillin the cat (Massimo Avoli & Gloor, 1981; M. Avoli et al., 1983), leading to the hypothesis that hypersynchrony in the spindle oscillations can result in SWDs that is a hallmark of absence seizures as well as other forms of epilepsy.

The transition from spindles to SWDs shown on EEG is indicative of epileptic seizure development, and previous studies have demonstrated that both the cortex and the thalamus are involved in this process (M. Avoli et al., 1983; Vergnes et al., 1987; Buzsáki et al., 1990; Avanzini et al., 2000; Slaght et al., 2002). The thalamocortical network consists of neocortical, thalamocortical neurons (TCNs), and the GABAergic thalamic reticular neurons (RENs) (Steriade et al., 1993; Thierry Bal & McCormick,

1996). TCNs are glutamatergic neurons and the key communicating component that connects the thalamus to cortex; specifically, they are connected to RENs, pyramidal neurons (PYNs) in the cortex, as well as cortical interneurons (IN) through AMPA- and GABAergic synapses (see Figure 1). TCNs also receive inhibitory input via GABAergic synapses from the reticular nucleus, and the glutamatergic PYNs of the cortex are reciprocally connected to the TCNs. This thalamocortical feedback loop largely contributes to the synchronization of cortical oscillations (Timofeev et al., 2012).

Previous investigations of the thalamocortical network suggested cortical neurons can trigger transitions between spindle and SWDs (Bazhenov et al., 2002; Polack et al., 2007). Other studies have illustrated that the reticular nucleus and TCNs are sufficient to produce spindles, and they also play an important role in SWDs development (Inoue et al., 1993; Pinault et al., 2001; Slaght et al., 2002). Notably, the firing activities of TCNs have been found to be closely time-correlated to SW seizures in related neocortical areas, and the inhibition of TCNs was mediated by GABAergic RENs (Steriade & Contreras, 1995), leading to the hypothesis that RENs are the ultimate pacemakers in the thalamocortical network. The exact mechanism for the oscillation frequency changes in the brain, however, remains poorly understood.

Thalamic network dynamics

In general, oscillatory activities in the brain are generated by intrinsic neuronal membrane properties and synaptic interactions of complex systems (Steriade, 2001). Recent studies on the thalamic network have demonstrated that TCNs are themselves neuronal oscillators that contribute to oscillations that propagate globally to affect brain states (reviewed in Fogerson & Huguenard, 2016). Recent studies have also shown that

the characteristic activities of the TCNs can initiate seizure generation. TCNs display either phasic or tonic firing activities depending on the brain states (Llinás & Jahnsen, 1982; Jahnsen & Llinás, 1984; Deschenes et al., 1984; Steriade et al., 1993). Interestingly, the synchronous phasic firing of TCNs initiates absence seizures, whereas the tonic firing of TCNs can terminate seizures (Sorokin et al., 2017).

RENs control spindles

Computer simulations and experimental studies on properties of RENs have shown support for their involvement in modulation of oscillation rhythms (Mulle et al., 1986; Huguenard & McCormick, 1992; Huguenard & Prince, 1994; Lytton et al., 1997; Slaght et al., 2002; Fan et al., 2017; McCafferty et al., 2018). Spindle oscillations as well as rhythmic IPSPs in TCNs were no longer observed without innervations of RENs, supporting the theory that RENs are spindle-oscillation pacemakers (Steriade et al., 1985). Indeed, deep-brain-stimulation studies have shown that high-frequency stimulation to the RE nucleus effectively interrupted abnormal synchronization in the thalamocortical circuit and had anti-epileptogenic effects, suggesting hyper-synchronization within the TCN circuit can be disrupted to prevent seizure generation (Pantoja-Jiménez et al., 2014; Wang & Wang, 2017; Magdaleno-Madrigal et al., 2019). Therefore, elucidating intra-thalamic membrane and synaptic mechanisms is important to understand the transitions of rhythmic oscillations underlying pathological brain states.

As illustrated in Figure 1, TCNs and RENs are reciprocally connected via AMPA- and GABAergic synapses. The participation of AMPA receptor-mediated currents at glutamatergic synapses in seizures have previously been studied. In the DBA/2 mouse model of audiogenic seizures and the WAG/Rij rat model of genetic absence seizures,

intraperitoneal injection of AMPA receptor antagonists had a significant anticonvulsant effect with relatively low toxicity (Peeters et al., 1994; Grasso et al., 1999; Jakus et al., 2004; Citraro et al., 2006, 2017; Zavvari et al., 2020). In adult GAERS rats, which is another well-recognized model of absence seizures, elevated expression of AMPA receptor proteins in the somatosensory cortex have been observed when compared with juvenile GAERS rats, which potentially contributes to the hyper-excitability of cortical neurons (Kennard et al., 2011). This is consistent with increased glutamatergic AMPA receptor expression in the peri-oral somatosensory cortex found in WAG/Rij rats compared to non-epileptic strains, and that AMPA receptor containing neurons in the reticular thalamic nucleus of WAG/Rij rats contribute to the synchronization of cortical and thalamic neurons (van de Bovenkamp-Janssen et al., 2006). Additionally, Gria4 gene encodes one of the four AMPA receptor subunits, and *Gria4* knockout mice show frequent SWDs, indicating that altered AMPA receptor subunit expression in mice might be involved in pathological synchronization oscillations (Beyer et al., 2008). Together, this information leads to the hypothesis that glutamatergic AMPA receptors might contribute to pathological thalamocortical network synchronization.

GABA receptors involved in oscillations: experimental evidence.

In addition to excitatory AMPA receptors, inhibitory inputs in the network mediated by $GABA_A$ and $GABA_B$ receptors were also extensively studied and appear to have different effects on the oscillatory activities. Mechanistically speaking, presynaptic inhibition mediated by activation of $GABA_B$ receptors reduces both GABA and glutamate release in many areas of the brain, and the activation of postsynaptic $GABA_B$ receptors located in the dendritic spines induces slow hyperpolarization in the

postsynaptic neuron (reviewed in Sanchez-Vives et al., 2021). Application of GABA$_A$ receptor antagonists in the thalamic relay nuclei transformed spindle oscillations into SWDs, although the transition was not observed in presence of both GABA$_A$ and GABA$_B$ receptor antagonists (Bal et al., 1995; Staak & Pape, 2001), suggesting that GABA$_B$ receptors may play a critical role in the transformation. Indeed, intraperitoneal injection of GABA$_B$ receptor antagonists, on the other hand, reduced the number and duration of SWDs (Puigcerver et al., 1996). These results suggest that both GABA$_A$ and GABA$_B$ receptors participate in mediating network frequencies, and GABA$_B$ receptor activation contributes significantly to hyper-synchronization.

Computational models

Computational models based on experimental data can provide theories on the dynamics of neural networks that drives future experimental inquiries. To model the role of various components of the TC circuit, computational models have also been developed. One study that used a single-compartment TC neuron model based on realistic channel conductance values showed that the interactions of different channel conductance controls both the resting membrane potential and the intrinsic oscillatory behavior of TC neurons (Amarillo et al., 2014). Another computational model consists of thalamic and cortical neurons based on biophysical data was developed and refined to investigate the complex interactions between synaptic mechanisms and the intrinsic neuronal firing properties (Destexhe et al., 1994; Destexhe, 1998; Destexhe et al., 1998). According to this model, increased cortical excitability could result in GABA$_B$-mediated inhibition in the thalamic circuit and force it into slower oscillations, which in turn caused SWDs in the cortex via the thalamocortical feedback loop. Further investigations on the oscillation

frequency transition mechanism based on this model revealed that spindle oscillations could be converted into SWDs by decreasing cortical GABA$_A$ conductance or increasing T-type calcium channel conductance; interestingly, activities of TCNs and RENs under spindle oscillations seem to be synchronized when they fire SWDs (Figure 2) as shown on raster plots based on data generated from the model (Knox et al., 2018). The phenomenon that TCNs fire in two clusters during spindle but fire in synchrony during SWDs is worth exploring via mathematical analysis.

Phase-response curve (PRC) theory

PRC theory is a powerful tool that can be used to predict whether a network of neurons will fire in synchrony. A regularly spiking neuron can be viewed as an oscillator, and a PRC of this neural oscillator can reflect how this neuron's spike time changes in response to small perturbations (Stiefel & Ermentrout, 2016). There are two types of PRCs; a neural model with Type I PRC will always advance its phase (causing the neuron to fire sooner) in response to a small positive voltage perturbation, whereas a neural model with Type II PRC can either advance or delay its phase (i.e., causing the neuron to fire sooner or later) depending on when in the phase that the small perturbation is applied (Hansel et al., 1995; B. Ermentrout, 1996; Brown et al., 2004). The biological definition of a PRC is that it describes the response of a neural oscillator to the input that it will receive in the network (C. C. Canavier & Achuthan, 2010). PRCs can provide accurate predictions on whether a system of more than one spiking neuron will fire in synchrony (Achuthan & Canavier, 2009; C. C. Canavier et al., 2009).

Based on the predictive property, PRC analysis has been applied in experimental neuroscience and has shown consistent and promising results with the computational

models. For example, carbachol-induced oscillations in hippocampal CA3 neurons in rats displays biphasic PRCs, a property that is consistent with *in vitro* observations that extracellular stimulus arriving before the trough of the local field potential advances the phase but delays during the rest of the cycle (Akam et al., 2012). Importantly, changes in ionic currents have been shown to produce a qualitative change in the shape of PRCs and the synchronization properties (B. Ermentrout et al., 2001; Hansel et al., 1995; Oprisan et al., 2004). Furthermore, changes in conductance of synaptic receptors located on a neuron can not only alter the shape of PRC, but also influence the neural coding capabilities (G. B. Ermentrout et al., 2007; Ratté et al., 2013). Cholinergic action in layer 2/3 PYNs in cortical slices caused a qualitative switch in the PRC type, and this switch ultimately implied a change in the spike generation mechanism though changes in slow voltage-dependent potassium currents such as the M-current (Stiefel et al., 2008). PRC theory bridges the theoretical and experimental work together, so utilizing PRC could help predict and determine mechanistic determinants of network synchronization properties. The hypothesis is that PRC theory can be applied to neurons, including physiologically bursting RENs, in the thalamocortical network to provide a theoretical explanation of frequency changes.

The current project

From the previous review, it is clear that (1) the thalamocortical network can transition between normal spindle and pathological SWDs oscillations; (2) the complex interactions between neurons in this network based on intrinsic and synaptic properties give rise to different oscillation modes; (3) conductance of AMPA and GABA receptors will affect the frequency of oscillations; (4) the thalamic circuit is crucial to

understanding the observed frequency changes; and (5) computational methods can be used to provide some mathematical explanations regarding the oscillation mechanism.

The goal of this project is to examine specific network-level effects associated with conductance changes of receptors and to determine if perturbations in this circuit can be modeled using phase resetting analysis. The computational model of the thalamocortical circuitry used in Knox et al. (2018) is perfectly suited to achieve this goal. The current project is mainly divided into two parts. The first part of the current project seeks to explore oscillatory frequency changes associated with varying synaptic conductance in the thalamocortical network. The second part of the current project focuses specifically on the RE-TC feedback loop, and changes in the burst timing after receiving perturbations are analyzed using phase resetting curves. These aims are important, because the ability to predict firing frequencies based on the factors that allow neurons to fire in clusters of different sizes is important to understand mechanisms of diseases associated with neuronal firing hypersynchrony, namely epilepsy.

Methods

Receptor conductance and oscillations

All simulations are run on a MacBook Pro using the NEURON simulator. The computational model of the thalamocortical network was originally developed by (Destexhe et al., 1998) and implemented by Knox et al. (2018), and this model will be referred to as the Knox model (available at http://senselab.med.yale.edu/ModelDB/showModel.cshtml?model=234233). Briefly, the Knox model consists of 100 of each of the following cell types: PYNs and IN (cortical) and TCNs and RENs (thalamic). Each type of neuron has a chain architecture, and there

are 100 neurons of each type in each layer, with excitatory and inhibitory synaptic connections between them. Each of the neurons has a single compartment with a resting potential determined by both intrinsic and postsynaptic currents. This model has cell type specific current dynamics based on experimental data and network specific excitatory and inhibitory connections between the cells.

Detailed descriptions on sources of the experimental data for synaptic and intrinsic currents in each type of neuron were described previously (Destexhe et al., 1998). Here, we focus on the conductance of specific receptors. A summary of previously determined ranges of various receptor conductance values that affected the oscillations in the network is listed in Table 1 (Destexhe, 1998). As illustrated in Figure 1, the excitatory connections (TC to RE, TC to IN, TC to PY, PY to PY, PY to IN, PY to RE, PY to TC) are mediated by AMPA synapses in the Knox model. The inhibitory connections (RE to TC, IN to PY) are mediated by a mixture of $GABA_A$ and $GABA_B$ receptors. The intra-RE connections are mediated by $GABA_A$ receptors. For each simulation, the stimulus was applied after the network has come to a steady state. This process takes about 10 seconds following the start of the last spontaneous oscillation.

We first tested the effects of changing the conductance of AMPA receptors located on RENs that receive excitatory input from PYNs in the Knox model. After the network reaches a steady state for each simulation, we applied a depolarizing current of -0.7 µA for 100 ms to a group of 5 PYNs to drive the network oscillations. As we mentioned earlier, neurons in the Knox model are organized in a chain architecture. Each type of neurons with indexes of 1 through 6 as well as 96 through 100 (end neurons) receive the same inputs from its neighboring neurons twice to preserve the chain

architecture. Figure 3A demonstrates a sample network connectivity of the second TCN and the second REN. It is clear from this illustration that they have doubling connections to its neighboring neurons, and this architecture might cause some undesirable end effects in the network. To this end, the network connectivity was altered from the original chain to a ring architecture to solve the issue with doubling connections. Specifically, instead of connecting these end neurons with its neighbors, we now have connected the ends to each other so that each neuron in this model receives only one input from each presynaptic neuron. Figure 3B illustrates the re-wired connections of the second TCN and the second REN that now displays network connectivity in a ring structure.

In the next set of simulations, we simplified the Knox model with chain architecture into two groups: cortical neurons, and the thalamic neurons. We treat INs and PYNs as one oscillating unit. Another oscillating unit is made up of TCNs and RENs. These two clusters of neurons communicate to each other via glutamatergic AMPA synapses between PYNs and TCNs. A network illustration of this simplified model is shown in Figure 7A. The same stimulus parameter as the one used in the previous set of simulations in the Knox model was applied after reaching steady state.

As mentioned in the introduction section, activities of TCNs and RENs are important in modulating rhythms of oscillation. To test the hypothesis that RENs are the ultimate pacemakers in the thalamocortical network, the synapses between the cortex and the thalamus were removed from the model to see if the TC-RE network would oscillate independently of the cortex. We then have further simplified the Knox model into a decorticated model: the model now only contains a RE-TC feedback loop made up of the TCNs and RENs as well as the connections between them. The schematic diagram is

shown in Figure 8A. The conductance strengths of $GABA_A$, $GABA_B$, and AMPA receptors within this simplified, decorticated model were subsequently altered to explore their effect upon thalamic dynamics. Since the cortex no longer innervates TCNs or RENs, a hyperpolarizing stimulus of -0.1 μA was applied for 100 ms on a group of 20 TCNs after reaching steady state.

PRC Analysis

To provide a simple mechanistic explanation of how synchronization arises in the thalamocortical network and how it can be disrupted, the PRC theory was used under the assumption of pulsatile coupling. In other words, we assumed that the communication between neurons through action potentials in this network are instantaneous. In this study, a unit burst oscillator is represented by a single neuron that is a reduced model of physiologically bursting neurons. We further assumed that the inputs of neurons from outside of each cluster are responsible for burst initiation and termination due to receptor conductance changes. We then hypothesized that RENs are particularly important for maintaining synchronized activities in the RE-TC network which in turn affects cortical synchronizations.

To apply PRC theory to the neural oscillators in the circuit, we first need to find an optimal parameter to get sustained and periodic firing of neurons in the thalamocortical circuit. We first tested whether changes in receptor conductance can produce such oscillations. Then, we applied the stimulus throughout the simulation to see if we can induce rhythmic oscillations. TCNs fire in clusters for spindle oscillations, whereas they fire in synchrony for SW oscillations. Consequently, the bursting activities of RENs display similar patterns. RENs split into clusters that display different burst

durations during spindle oscillations, but populations of RENs with varying burst

durations start firing in synchrony during SW. The individual TCN and REN are treated

as oscillators on their own, and all neurons that are within the same cluster are considered

identical. Therefore, a regularly bursting REN was tested and analyzed since we assumed

that RENs within the same cluster are all identical.

We further reduced the decorticated model into a model of single REN and a

model of a single REN reciprocally connected to a single TCN to induce rhythmic

oscillations suitable for PRC analysis. For each PRC generated, the first spike of the

presynaptic neuron was applied at different phases of the period of the postsynaptic RE

neuron for which the PRC was being measured. The phase, denoted as φ, is quantified as

the fraction of an intrinsic period [0,1] that has elapsed. The intrinsic period, denoted as

P_0, is defined as the time that has elapsed until right before the onset of the next burst

since the most recent start of the burst. The perturbed period, denoted as P_1, has the same

definition as the intrinsic period P_0. The amount of resetting, denoted as $f(\varphi)$, is defined

as the difference between a perturbed period and the intrinsic period normalized by the

intrinsic period. The normalized change in the cycle period is obtained using the

following equation:

$$f(\varphi) = \frac{P_1 - P_0}{P_0}$$

Therefore, a positive resetting means that the onset of the next burst is delayed, and a

negative resetting means that the onset of the next burst is advanced. Starting from any

initial phase $\varphi(n)$ where a perturbation is received, the evolution of the phase on

successive perturbation index, i, with a total number of perturbations applied, N, is

obtained using the following equation:

$$\varphi(n) \ = \frac{\frac{P_0}{N} \times i}{P_0}$$

Once transients have died out, a square depolarizing current with an amplitude of

0.06 μA was applied to this single REN and lasted throughout the simulation. The first

set of small perturbations used to generate a PRC in this model are a train of depolarizing

current pulses (100 total) with an amplitude of 0.1 μA and a duration of 1 ms. Since

RENs are interconnected with inhibitory $GABA_A$ synapses from neighboring RENs, the

effect of that one REN firing has on the other REN firing was then explored. In order to

predict the network activity, perturbations that will be received in the circuit were used

instead of a random current stimulus. This set of small perturbations used was driven by

the conductance delay of $GABA_A$ receptor located on the REN.

A similar approach was used in another model consists of single pair of TC-RE

neurons were made to provide a more accurate estimation based on circuit-level effect.

Just as the single REN model, a current clamp with an amplitude of 0.06 μA was applied

to the REN in this model and lasted throughout the simulation. We first generated a PRC

for TCN using the conductance of both $GABA_A$ and $GABA_B$ receptors located on the

TCN. Then, we generated PRCs for the REN with perturbations based on AMPA

receptor conductance delay, AMPA as well as intra-RE $GABA_A$ receptor conductance

delay, and an intra-RE $GABA_A$ receptor conductance delay.

Results

Effects of AMPA receptor conductance changes in the complete Knox model

To examine the specific network-level effects associated with synaptic conductance

changes in the thalamocortical network, we first changed the conductance of AMPA

receptors located on RENs that receive excitatory input from PYNs. Table 2 shows a summary of the conductance values tested in this model under spindle conditions. We found that reducing the conductance of PY→RE AMPA receptors did not change the clustering or frequency in TCNs, but it prolonged the activity of some TCNs (Figure 4B). Increasing the conductance of PY→RE AMPA receptors, however, caused TCNs to form different clusters, and a higher degree of synchronization in TCNs can be observed (Figure 4C and 4D). These results showed that the excitability of RENs might be important to control the network activity. Even though these are transient results, TCNs seem to take longer to breakdown after increasing the conductance of PY→RE AMPA receptors.

Changing the network architecture did not affect frequency or clustering

Neurons in the Knox model are connected through a chain architecture. As we mentioned previously in the methods section, the end neurons of each type must receive doubling input from its neighbors to preserve the chain architecture. The issue with the current network architecture is that the activities of these end neurons might be different than neurons located more towards the center. To get rid of the end effects, we changed the network connectivity such that each neuron receives only one input from other neurons (Figure 3B). Figure 5 shows the raster plots for TCNs and RENs in the Knox model with a chain architecture under optimal spindle and SW oscillation parameters. To confirm that this connectivity change did not produce any confounding effects, we used the same stimulus parameter as the one used for producing Figure 5. Comparing Figure 5A with Figure 6A, the oscillation frequency and clustering in the ring architecture does

not differ significantly from those in the chain architecture during spindle oscillations; the same effect is observed during SWDs when comparing Figure 5B with Figure 6B.

Effects of receptor conductance changes in the simplified model

To answer the question on how exactly the frequency transition happens within the thalamocortical circuit, we simplified the Knox model with a chain architecture by treating cortical neurons, INs and PYNs, as one oscillating unit and thalamic neurons, TCNs and RENs, as the other oscillating unit. Since TCNs and PYNs both receive from and send excitatory input to each other, we preserved the glutamatergic AMPA synapses between them so that these two clusters can communicate with each other. The network schematic diagram is shown in Figure 7A. In this set of simulations, we specifically focused on testing the effects of changing conductance of AMPA receptors located on both TCNs and PYNs as well as the conductance of GABA$_A$ receptors located on PYNs. Table 3 shows a summary of parameters tested in this reduced network, although the results for changes of conductance of AMPA receptors located on TCNs (PYNs are the presynaptic neurons) were omitted as no significant difference on the network frequency was observed.

Figure 7B is the control figure that used the optimal conductance values under SWD conditions. Despite having the characteristic "C" shape of firing bands, the frequency of firing is about the same comparing with Figure 2B. This shows that this reduced model is still an appropriate simplification. As expected, reducing the conductance of IN→PY GABA$_B$ receptors (Figure 7C) or increasing the TC→PY AMPA receptor conductance (Figure 7D) prolonged the firing activities and made a greater number of neurons become more excitable, but a change in firing frequency or clustering

in TCNs was not observed. Increasing the TC→PY AMPA receptor conductance with a reduced conductance of GABA$_A$ synapses between IN and PYNs yields the same effect (Figure 7E and 7F). Changing conductance receptors in a circuit where RENs were not innervated by the cortex did not change the frequency or clustering in each type of neurons.

Effects of receptor conductance changes in the decorticated RE-TC thalamic network

Previous literature demonstrated the importance of TCNs and RENs in modulating oscillation rhythms. Since we hypothesized that RENs are the ultimate pacemakers in the thalamocortical network, we further reduced the model by fully removing the connections between the cortex and the thalamic neurons to obtain a simplified model composing of only 100 of RENs and TCNs. Figure 8B shows the activities of PYNs, RENs, and TCNs under optimal receptor conductance. Since we did not include PYNs in this reduced model, we are expected to see no activities in the panel for PYNs since they should all be at rest. Comparing Figure 8B with Figure 2B, the activities of the neurons in this decorticated RE-TC thalamic network are similar to the ones in the full model. Therefore, this reduction in the model should be appropriate for determining how activities of RENs are affected by the conductance changes.

Table 4 shows a summary of parameters tested in the decorticated RE-TC thalamic network. We first observed that changing conductance of GABA receptors within the thalamus without cortical input does not contribute to sustained clustering in TCNs. Decreasing intra-RE GABA$_A$ receptor conductance helped with sustaining the activities of a small fraction of TCNs (Figure 8C), but no significant changes on the frequency or clustering in either populations were observed. Consistent with the

inhibitory effect of GABA$_A$, increasing the conductance for GABA$_A$ receptors attenuated the firing activities of RENs (Figure 8D).

Reducing both intra-RE GABA$_A$ and RE→TC GABA$_A$ receptors conductance contributes to a more synchronized firing pattern for RENs, but activities of TCNs and RENs both attenuated after about 2.5 seconds (Figure 8E). We were able to induce spindle oscillations in the decorticated model as shown in Figure 8E. Additionally, two clusters of different sizes alternatively fired in TCNs briefly, with the smaller cluster (groups of 1 single TCN) stopped firing before the bigger cluster (groups of about 3 TCNs) was shown on the raster plot (Figure 8F). Compared with Figure 8D, increasing RE→TC GABA$_A$ receptor conductance in addition to increasing the conductance of intra-RE GABA$_A$ receptors surprisingly prolonged the firing activities of RENs (Figure 8G).

Changes in RE→TC GABA$_B$ receptor conductance had opposite effects as changing the RE→TC GABA$_A$ receptor conductance. Decreasing the conductance of GABA$_B$ receptors located on TCNs stops both TCNs and RENs from firing earlier (Figure 9A) compared with the control (Figure 8B). However, increasing RE→TC GABA$_B$ receptor conductance excites RENs and prolonged firing in both populations of neurons (Figure 9B). Further increasing the conductance of RE→TC GABA$_B$ receptors in this model appears to contribute to stronger synchronization of firing activities in both RENs and TCNs.

AMPA receptors located on RENs in this model might contribute to clustering in TCNs. As expected, reducing the conductance of AMPA receptors made neurons less excitable (Figure 10A). As we increase TC→RE AMPA receptor conductance, the

frequency and duration of neuronal firing increases (Figure 10B through 10D). Both

TCNs and RENs appear to favor the transition pattern as the conductance of AMPA

receptors, and less synchronization can be observed in this model. Consistent with our

hypothesis that AMPA receptors located on RENs might give rise to their pace-making

capability, changing the conductance of AMPA receptors located on RENs appears to

have the greatest effect on network activities in the decorticated model.

Applying stimulus throughout the simulation triggered sustained oscillations

To see if phase resetting theory can account for the frequency transitions, we first

need to find an optimal parameter such that the oscillations are sustained and periodic

rather than transient. Unfortunately, none of the manipulations of the conductance values

that we tested in any of the above-mentioned models produced oscillations that meet the

requirement for PRC analysis. We then tested different stimulus parameters to see if we

could get sustained oscillations in the network. Figure 11A illustrates the raster plots of

TCNs and RENs under optimal receptor conductance for spindle oscillations with the

same stimulus used in the decorticated model from the first part of this study. We

prolonged the stimulus applied on the same group of TCNs, and we were able to produce

sustained oscillations in this circuit (Figure 11B). Specifically, right after stimulating a

group of 20 TCNs with a hyperpolarizing current of -0.1 μA for 100 ms, we continued

stimulating them with a depolarizing current of 1.0 μA until the end of the simulation.

To test the hypothesis that RENs are particularly important for maintaining

synchronized activities in the RE-TC network, we focused on testing whether we can

induce rhythmic oscillations in RENs. With a constant depolarizing current of 0.1 μA

applied on all RENs, they seem to be bursting spontaneously (Figure 12A). Interestingly,

the traveling wave effect in the population of RENs in the decorticated network changes with the altered connectivity (Figure 12B), although the burst duration and clustering remained the same despite having the same stimulus and parameter regime as used in Figure 12A.

We then increased the amplitude of the current stimulus to 0.3 µA. With this slightly larger depolarizing current, RENs appear to fire mostly in groups of twos after reaching steady state (Figure 13). In addition, increasing the τ_0 value increases the burst duration and changes the traveling wave effect. In Figure 13B, specifically, after a group of two RENs fires, the next group of two RENs with the next lowest index number fires despite having no intra-RE GABA$_A$ receptor conductance delay. Their TCNs pairs stopped firing after about 500 ms after stimuli being applied, so they did not produce sustained firing activities (figure not shown). Since each REN is connected to its neighbors on both sides, a novel mechanism of refractory process might exist to prevent the pair of RENs from firing at the same time with the next pair of RENs. RENs located on both the ends of the chain are more likely to switch their firing partners, and this complicated pattern exists most likely due to the fact that these neurons receive the same input twice from their neighbors.

PRC Analysis

Based on the previous analysis, a constant depolarizing current applied to all RENs in the decorticated network of TCNs and RENs can induce sustained oscillations of similar clusters. However, the consistent periodic firing of one or two clusters in each type of neuron was not observed. Therefore, to simplify the network effect, we then further reduced the RE-TC network into a model of single REN to look at effects of intra-

RE connections, and a model of a single REN reciprocally connected to a single TCN to look at the effects of RE-TC connections. We assumed that our model neurons are representative of neurons within the same cluster. By perturbing the model neuron at each point of the firing cycle (starting from the onset of burst to right before the next burst imitation) and recording the time of the onset of the next burst, six different PRCs for each spindle and SW parameters (so a total of 12 PRCs) were generated to provide reliable estimations on whether the next burst is advanced or delayed.

In the single REN model, application of the square depolarizing current with an amplitude of 0.06 µA triggered sustained and rhymical burst firing of our modeled REN under SWD parameters ($\tau_0 = 50$). Figure 14A shows the voltage trace of the modeled REN, and the first 1500 ms of the simulation was discarded, as no stimulation was applied during that period to allow the model to reach as stabilized state. Figure 14B is the voltage trace of REN with an index number of 40 in the original Knox model under SWD parameters for comparison. The period used for PRC analysis begins at the onset of the third burst (t $\approx$ 1800 ms, $\varphi = 0$) and ends right before the onset of the fourth burst ((t $\approx$ 2700 ms, $\varphi = 1$).

For the PRC shown in Figure 14C, the perturbations used was depolarizing current (I = 0.06 µA) pulses, and each pulse lasts for only 1 ms. The resulting PRC displays a sinusoidal shape with both positive and negative lobes, meaning that depending on the timing of the input during the period, the next burst can either be advanced or delayed. The voltage traces at $\varphi = 0.5$ and at $\varphi = 0.8$ shows advance and delay, respectively, of the next onset of a burst. Note that the x-axis did not begin with a zero, and 1500 ms needs to be subtracted to get the exact time stamp of the onset of the

next burst after perturbation. Similarly, we generated another PRC with perturbations that are based on intra-RE GABA$_A$ conductance (Figure 14D) and showed voltage traces at advance ($\varphi = 0.4$) and delay ($\varphi = 0.8$) periods. The PRC generated based on the conductance of intra-RE GABA$_A$ receptors displays a different shape, although it also displays the biphasic property based on the values of $f(\varphi)$. In the set of simulations of this single REN model ran under spindle parameters (Figure 15, $\tau_0 = 28.3$, $\varphi = 0$ at t $\approx$ 1600 ms, $\varphi = 1$ at t $\approx$ 2400 ms), similar effects were observed. Notably, comparing the unperturbed voltage traces of the modeled REN, the burst duration is much shorter, but the amount of resetting appears to be of greater range.

In a single pair of mutually connected RE-TC neurons model, the voltage traces of REN and TCN resembled the traces observed in the Knox model closer. Note that the first 4000 ms of each simulation ran in this model was discarded to allow for the network to come to stabilization. Each of the voltage trace at a specific phase of its respective PRC was not zeroed so the x-axis began at 6400 ms instead of 2400 ms. The period we selected for analysis begins at the onset of the fourth burst and ends right before the onset of the next burst for both REN and TCN under both spindle and SWD parameters. The depolarization-driven PRCs are omitted, because they do not offer physiological insights to network-level effects.

Figure 16 shows the results obtained from simulations ran under SWD parameters. Figure 16D displays the PRC generated for REN based on both AMPAergic inputs from TCN and GABAergic inputs from other REN. The green arrow points at a specific voltage trace ($\varphi = 0.3$) during the advance phase, and the red arrow points at a specific voltage trace ($\varphi = 0.8$) during the delay phase. To look at the effect of each type

of the receptor, two other PRCs were generated for REN (Figure 16E and Figure 16F). Interestingly, the shape of PRC with a GABA$_A$ receptor-driven perturbations is very similar to the previous PRC, and the voltage traces at $\varphi = 0.3$ in both cases are also similar. At $\varphi = 0.3$ of the AMPA receptor-driven PRC, a burst was triggered during time that the set of perturbations was applied, and the onset of the next regular burst was delayed. From the GABAergic input-driven PRC for TCN, (Figure 16G) perturbations during the period always delays the onset of the next spike.

The results of simulations ran under spindle parameters in the RE-TC pair model are summarized in Figure 17. Consistent with more spikes each time that the TCN fires in the Knox model (Figure17C), more spikes are also observed each time the TCN fires (Figure 17B). Comparing with the shape of GABA$_A$ receptor-driven PRC, the shape of PRC generated for REN using AMPA and GABA$_A$ receptor conductance (Figure 17D) is much more similar to the shape PRC generated using AMPA receptor conductance alone (Figure 17F). Additionally, the GABA receptor conductance-driven PRC for TCN (Figure 17G) now displays biphasic property.

Discussion

In the present study, we analyzed how changes in the conductance of postsynaptic receptors affects the firing activities of neurons in the thalamocortical circuit. We mostly focused on the decorticated RE-TC thalamic circuit in our analysis, and we were able to generate PRCs to determine how the next onset of firing would be affected depending on the timing of the perturbations.

Our results support the hypothesis that RENs might be the ultimate pacemakers in the thalamocortical network, and that glutamatergic AMPA receptors might contribute to

pathological thalamocortical network synchronization. We showed that changes in conductance of AMPA receptors located on RENs that receive inputs from PYNs affect the synchronization and firing duration in TCNs but does not affect the frequency of firing. We also showed that increasing the conductance of AMPA receptors located on RENs that receive inputs from TCNs could in turn increases the frequency and duration of firing in the thalamocortical circuit. Our results on AMPA receptor conductance changes are consistent with the experimental result that the Gria4 knockout mice display frequent SWDs (Beyer et al., 2008), suggesting a reduced AMPA receptor conductance leads to a decrease in the frequency of synchrony of oscillations. However, further investigation is necessary.

We also found that changes in conductance of $GABA_A$ and AMPA receptors located on PYNs may prolong the firing durations in most neurons in the thalamocortical circuit, but no significant changes in frequency or synchronization was induced without innervations of RENs; additionally, changes in conductance of GABAergic synapses between TCNs and RENs affects the firing duration. Specifically, experimental findings showed that activation of postsynaptic $GABA_B$ receptors affects rhythmic firing as well as synaptic plasticity (reviewed in Sanchez-Vives et al., 2021); our results shown in Figure 9 is consistent with the finding in that changing the conductance of $GABA_B$ receptors appears to contribute to stronger and more stable synchronization of firing activities in thalamic neurons.

From the PRC analysis on the intra-RE connections, we found that RENs can either trigger the next burst sooner or later depending on the timing of the input that they receive. Depending on how many simultaneous inputs that RENs are receiving from, the

PRCs would look differently. The most relevant PRCs are illustrated in Figure 14D, 15D, 16D, and 17D, as they were generated using proper synaptic conductance delays based on activation times during the unperturbed period. For the same perturbations that each REN receives, there is a greater amount of resetting when RENs are firing under spindle than under SWD oscillation parameters. This might partially explain the greater number of bursts observed in RENs during spindle oscillations than during SWD. Additionally, $GABA_A$ receptor-mediated currents might be dominant the effect on the firing activities of RENs during SWD, but during spindles the conductance of AMPA receptor-mediated currents might be more important.

One limitation of the current study is that we did not test more combinations of different conductance values of receptors in all three versions of the model. Additionally, performing a Fast Fourier transformation (FFT) analysis of PYNs for each simulation in the Knox model and the reduced model would provide a much more reliable indication on the frequency. The frequency changes observed in our current study were based on simple qualitative estimation by looking at the heat plots, so FFT analysis could provide a much more objective and quantitative result on the frequency changes.

Another limitation in our PRC analysis is that we did not perform a stability analysis. A stability analysis using the slopes of PRCs should be done in any future work extending from the current project, as it could help to provide more insights on whether the network will fire in clusters or in synchrony. A negative slope or any positive slope greater than 2 at a point on the PRC means that the input at this specific phase is destabilizing. For Figure 14D, the conductance value for $GABA_A$ receptor we used was the same as the optimal intra-RE $GABA_A$ receptor conductance. We did not try to

increase the RE-to-RE synaptic delay, but we might be able to use a synaptic delay of $\varphi = 0.05$ to skip the negative slope regions between approximately $\varphi = 0$ to 0.05. Previous studies have demonstrated how we can perform stability analysis using PRCs of neural oscillators to predict whether the clusters will synchronize (Goel & Ermentrout, 2002; Chandrasekaran et al., 2011; Woodman & Canavier, 2011; C. Canavier et al., 2013; Rich et al., 2016), which in our case could help to predict whether we would see the transition from spindle oscillations to SWDs.

In conclusion, this present study offered some insights on the mechanism of frequency transitions based on conductance-driven synchronization changes in the thalamocortical model. More work, however, still need to be done to provide more evidence to support the hypothesis that RENs are the ultimate pacemakers that governs the network synchronizations.

List of References

Achuthan, S., & Canavier, C. C. (2009). Phase-Resetting Curves Determine Synchronization, Phase Locking, and Clustering in Networks of Neural Oscillators. *Journal of Neuroscience*, *29*(16), 5218–5233. https://doi.org/10.1523/JNEUROSCI.0426-09.2009

Akam, T., Oren, I., Mantoan, L., Ferenczi, E., & Kullmann, D. M. (2012). Oscillatory dynamics in the hippocampus support dentate gyrus–CA3 coupling. *Nature Neuroscience*, *15*(5), 763–768. https://doi.org/10.1038/nn.3081

Amarillo, Y., Zagha, E., Mato, G., Rudy, B., & Nadal, M. S. (2014). The interplay of seven subthreshold conductances controls the resting membrane potential and the oscillatory behavior of thalamocortical neurons. *Journal of Neurophysiology*, *112*(2), 393–410. https://doi.org/10.1152/jn.00647.2013

Avanzini, G., Panzica, F., & de Curtis, M. (2000). The role of the thalamus in vigilance and epileptogenic mechanisms. *Clinical Neurophysiology*, *111*, S19–S26. https://doi.org/10.1016/S1388-2457(00)00398-9

Avoli, M., Gloor, P., Kostopoulos, G., & Gotman, J. (1983). An analysis of penicillin-induced generalized spike and wave discharges using simultaneous recordings of cortical and thalamic single neurons. *Journal of Neurophysiology*, *50*(4), 819–837. https://doi.org/10.1152/jn.1983.50.4.819

Avoli, Massimo, & Gloor, P. (1981). The Effects of Transient Functional Depression of the Thalamus on Spindles and on Bilateral Synchronous Epileptic Discharges of Feline Generalized Penicillin Epilepsy. *Epilepsia*, *22*(4), 443–452. https://doi.org/10.1111/j.1528-1157.1981.tb06155.x

Bal, T., Krosigk, M. von, & McCormick, D. A. (1995). Synaptic and membrane mechanisms underlying synchronized oscillations in the ferret lateral geniculate nucleus in vitro. *The Journal of Physiology*, *483*(3), 641–663. https://doi.org/10.1113/jphysiol.1995.sp020612

Bal, Thierry, & McCormick, D. A. (1996). What Stops Synchronized Thalamocortical Oscillations? *Neuron*, *17*(2), 297–308. https://doi.org/10.1016/S0896-6273(00)80161-0

Bazhenov, M., Timofeev, I., Steriade, M., & Sejnowski, T. J. (2002). Model of Thalamocortical Slow-Wave Sleep Oscillations and Transitions to Activated States. *Journal of Neuroscience*, *22*(19), 8691–8704. https://doi.org/10.1523/JNEUROSCI.22-19-08691.2002

Beyer, B., Deleuze, C., Letts, V. A., Mahaffey, C. L., Boumil, R. M., Lew, T. A., Huguenard, J. R., & Frankel, W. N. (2008). Absence seizures in C3H/HeJ and

knockout mice caused by mutation of the AMPA receptor subunit Gria4. *Human Molecular Genetics*, *17*(12), 1738–1749. https://doi.org/10.1093/hmg/ddn064

Brown, E., Moehlis, J., & Holmes, P. (2004). On the Phase Reduction and Response Dynamics of Neural Oscillator Populations. *Neural Computation*, *16*(4), 673–715. https://doi.org/10.1162/089976604322860668

Buzsáki, G., Smith, A., Berger, S., Fisher, L. J., Gage, F. H., Aston-Jones, G., & Bloom, F. E. (1990). Petit mal epilepsy and parkinsonian tremor: Hypothesis of a common pacemaker. *Neuroscience*, *36*(1), 1–14. https://doi.org/10.1016/0306-4522(90)90345-5

Byars, A. W., Byars, K. C., Johnson, C. S., deGrauw, T. J., Fastenau, P. S., Perkins, S., Austin, J. K., & Dunn, D. W. (2008). The relationship between sleep problems and neuropsychological functioning in children with first recognized seizures. *Epilepsy & Behavior*, *13*(4), 607–613. https://doi.org/10.1016/j.yebeh.2008.07.009

Canavier, C. C., & Achuthan, S. (2010). Pulse coupled oscillators and the phase resetting curve. *Mathematical Biosciences*, *226*(2), 77–96. https://doi.org/10.1016/j.mbs.2010.05.001

Canavier, C. C., Kazanci, F. G., & Prinz, A. A. (2009). Phase Resetting Curves Allow for Simple and Accurate Prediction of Robust N:1 Phase Locking for Strongly Coupled Neural Oscillators. *Biophysical Journal*, *97*(1), 59–73. https://doi.org/10.1016/j.bpj.2009.04.016

Canavier, C., Wang, S., & Chandrasekaran, L. (2013). Effect of phase response curve skew on synchronization with and without conduction delays. *Frontiers in Neural Circuits*, *7*. https://doi.org/10.3389/fncir.2013.00194

Chandrasekaran, L., Achuthan, S., & Canavier, C. C. (2011). Stability of two cluster solutions in pulse coupled networks of neural oscillators. *Journal of Computational Neuroscience*, *30*(2), 427–445. https://doi.org/10.1007/s10827-010-0268-x

Citraro, R., Leo, A., Franco, V., Marchiselli, R., Perucca, E., Sarro, G. D., & Russo, E. (2017). Perampanel effects in the WAG/Rij rat model of epileptogenesis, absence epilepsy, and comorbid depressive-like behavior. *Epilepsia*, *58*(2), 231–238. https://doi.org/10.1111/epi.13629

Citraro, R., Russo, E., Gratteri, S., Di Paola, E. D., Ibbadu, G. F., Curinga, C., Gitto, R., Chimirri, A., Donato, G., & De Sarro, G. (2006). Effects of non-competitive AMPA receptor antagonists injected into some brain areas of WAG/Rij rats, an animal model of generalized absence epilepsy. *Neuropharmacology*, *51*(6), 1058–1067. https://doi.org/10.1016/j.neuropharm.2006.06.014

Deschenes, M., Paradis, M., Roy, J. P., & Steriade, M. (1984). Electrophysiology of neurons of lateral thalamic nuclei in cat: Resting properties and burst discharges. *Journal of Neurophysiology*, *51*(6), 1196–1219. https://doi.org/10.1152/jn.1984.51.6.1196

Destexhe, A. (1998). Spike-and-Wave Oscillations Based on the Properties of GABAB Receptors. *Journal of Neuroscience, 18*(21), 9099–9111. https://doi.org/10.1523/JNEUROSCI.18-21-09099.1998

Destexhe, A., Contreras, D., Sejnowski, T. J., & Steriade, M. (1994). A model of spindle rhythmicity in the isolated thalamic reticular nucleus. *Journal of Neurophysiology*, *72*(2), 803–818. https://doi.org/10.1152/jn.1994.72.2.803

Destexhe, A., Contreras, D., & Steriade, M. (1998). Mechanisms Underlying the Synchronizing Action of Corticothalamic Feedback Through Inhibition of Thalamic Relay Cells. *Journal of Neurophysiology*, *79*(2), 999–1016. https://doi.org/10.1152/jn.1998.79.2.999

Ermentrout, B. (1996). Type I Membranes, Phase Resetting Curves, and Synchrony. *Neural Computation*, *8*(5), 979–1001. https://doi.org/10.1162/neco.1996.8.5.979

Ermentrout, B., Pascal, M., & Gutkin, B. (2001). The Effects of Spike Frequency Adaptation and Negative Feedback on the Synchronization of Neural Oscillators. *Neural Computation*, *13*(6), 1285–1310. https://doi.org/10.1162/08997660152002861

Ermentrout, G. B., Galán, R. F., & Urban, N. N. (2007). Relating Neural Dynamics to Neural Coding. *Physical Review Letters*, *99*(24), 248103. https://doi.org/10.1103/PhysRevLett.99.248103

Fan, D., Liao, F., & Wang, Q. (2017). The pacemaker role of thalamic reticular nucleus in controlling spike-wave discharges and spindles. *Chaos: An Interdisciplinary Journal of Nonlinear Science*, *27*(7), 073103. https://doi.org/10.1063/1.4991869

Fogerson, P. M., & Huguenard, J. R. (2016). Tapping the Brakes: Cellular and Synaptic Mechanisms that Regulate Thalamic Oscillations. *Neuron*, *92*(4), 687–704. https://doi.org/10.1016/j.neuron.2016.10.024

Goel, P., & Ermentrout, B. (2002). Synchrony, stability, and firing patterns in pulse-coupled oscillators. *Physica D: Nonlinear Phenomena*, *163*(3), 191–216. https://doi.org/10.1016/S0167-2789(01)00374-8

Grasso, S., De Sarro, G., De Sarro, A., Micale, N., Zappalà, M., Puia, G., Baraldi, M., & De Micheli, C. (1999). Synthesis and Anticonvulsant Activity of Novel and Potent 2,3-Benzodiazepine AMPA/Kainate Receptor Antagonists. *Journal of Medicinal Chemistry, 42*(21), 4414–4421. https://doi.org/10.1021/jm991086d

Hansel, D., Mato, G., & Meunier, C. (1995). Synchrony in Excitatory Neural Networks. *Neural Computation*, *7*(2), 307–337. https://doi.org/10.1162/neco.1995.7.2.307

Huguenard, J. R., & McCormick, D. A. (1992). Simulation of the currents involved in rhythmic oscillations in thalamic relay neurons. *Journal of Neurophysiology*, *68*(4), 1373–1383. https://doi.org/10.1152/jn.1992.68.4.1373

Huguenard, J. R., & Prince, D. A. (1994). Intrathalamic rhythmicity studied in vitro: Nominal T-current modulation causes robust antioscillatory effects. *Journal of Neuroscience*, *14*(9), 5485–5502. https://doi.org/10.1523/JNEUROSCI.14-09-05485.1994

Inoue, M., Duysens, J., Vossen, J. M. H., & Coenen, A. M. L. (1993). Thalamic multiple-unit activity underlying spike-wave discharges in anesthetized rats. *Brain Research*, *612*(1), 35–40. https://doi.org/10.1016/0006-8993(93)91641-5

Jahnsen, H., & Llinás, R. (1984). Electrophysiological properties of guinea-pig thalamic neurones: An in vitro study. *The Journal of Physiology*, *349*(1), 205–226. https://doi.org/10.1113/jphysiol.1984.sp015153

Jakus, R., Graf, M., Ando, R. D., Balogh, B., Gacsalyi, I., Levay, G., Kantor, S., & Bagdy, G. (2004). Effect of two noncompetitive AMPA receptor antagonists GYKI 52466 and GYKI 53405 on vigilance, behavior and spike–wave discharges in a genetic rat model of absence epilepsy. *Brain Research*, *1008*(2), 236–244. https://doi.org/10.1016/j.brainres.2004.01.087

Jankel, W. R., & Niedermeyer, E. (1985). Sleep spindles. *Journal of Clinical Neurophysiology: Official Publication of the American Electroencephalographic Society*, *2*(1), 1–35. https://doi.org/10.1097/00004691-198501000-00001

Kennard, J. T. T., Barmanray, R., Sampurno, S., Ozturk, E., Reid, C. A., Paradiso, L., D'Abaco, G. M., Kaye, A. H., Foote, S. J., O'Brien, T. J., & Powell, K. L. (2011). Stargazin and AMPA receptor membrane expression is increased in the somatosensory cortex of Genetic Absence Epilepsy Rats from Strasbourg. *Neurobiology of Disease*, *42*(1), 48–54. https://doi.org/10.1016/j.nbd.2011.01.003

Knox, A. T., Glauser, T., Tenney, J., Lytton, W. W., & Holland, K. (2018). Modeling Pathogenesis and Treatment Response in Childhood Absence Epilepsy. *Epilepsia*, *59*(1), 135–145. https://doi.org/10.1111/epi.13962

Kotagal, P., & Yardi, N. (2008). The Relationship Between Sleep and Epilepsy. *Seminars in Pediatric Neurology*, *15*(2), 42–49. https://doi.org/10.1016/j.spen.2008.03.007

Llinás, R., & Jahnsen, H. (1982). Electrophysiology of mammalian thalamic neurones in vitro. *Nature*, *297*(5865), 406–408. https://doi.org/10.1038/297406a0

Lytton, W. W., Contreras, D., Destexhe, A., & Steriade, M. (1997). Dynamic Interactions Determine Partial Thalamic Quiescence in a Computer Network Model of Spike-

and-Wave Seizures. *Journal of Neurophysiology*, *77*(4), 1679–1696. https://doi.org/10.1152/jn.1997.77.4.1679

Magdaleno-Madrigal, V. M., Contreras-Murillo, G., Valdés-Cruz, A., Martínez-Vargas, D., Martínez, A., Villasana-Salazar, B., & Almazán-Alvarado, S. (2019). Effects of High- and Low-Frequency Stimulation of the Thalamic Reticular Nucleus on Pentylentetrazole-Induced Seizures in Rats. *Neuromodulation: Technology at the Neural Interface*, *22*(4), 425–434. https://doi.org/10.1111/ner.12926

McCafferty, C., David, F., Venzi, M., Lőrincz, M. L., Delicata, F., Atherton, Z., Recchia, G., Orban, G., Lambert, R. C., Di Giovanni, G., Leresche, N., & Crunelli, V. (2018). Cortical drive and thalamic feed-forward inhibition control thalamic output synchrony during absence seizures. *Nature Neuroscience*, *21*(5), 744–756. https://doi.org/10.1038/s41593-018-0130-4

Mulle, C., Madariaga, A., & Deschenes, M. (1986). Morphology and electrophysiological properties of reticularis thalami neurons in cat: In vivo study of a thalamic pacemaker. *Journal of Neuroscience*, *6*(8), 2134–2145. https://doi.org/10.1523/JNEUROSCI.06-08-02134.1986

Oprisan, S. A., Prinz, A. A., & Canavier, C. C. (2004). Phase Resetting and Phase Locking in Hybrid Circuits of One Model and One Biological Neuron. *Biophysical Journal*, *87*(4), 2283–2298. https://doi.org/10.1529/biophysj.104.046193

Pantoja-Jiménez, C. R., Magdaleno-Madrigal, V. M., Almazán-Alvarado, S., & Fernández-Mas, R. (2014). Anti-epileptogenic Effect of High-frequency Stimulation in the Thalamic Reticular Nucleus on PTZ-induced Seizures. *Brain Stimulation*, *7*(4), 587–594. https://doi.org/10.1016/j.brs.2014.03.012

Peeters, B. W. M. M., Ramakers, G. M. J., Ellenbroek, B. A., Vossen, J. M. H., & Coenen, A. M. L. (1994). Interactions Between NMDA and NonNMDA Receptors in Nonconvulsive Epilepsy in the WAG/Rij Inbred Strain. *Brain Research Bulletin*, *33*(6), 715–718. https://doi.org/10.1016/0361-9230(94)90237-2

Pinault, D., Vergnes, M., & Marescaux, C. (2001). Medium-voltage 5–9-Hz oscillations give rise to spike-and-wave discharges in a genetic model of absence epilepsy: In vivo dual extracellular recording of thalamic relay and reticular neurons. *Neuroscience*, *105*(1), 181–201. https://doi.org/10.1016/S0306-4522(01)00182-8

Polack, P.-O., Guillemain, I., Hu, E., Deransart, C., Depaulis, A., & Charpier, S. (2007). Deep Layer Somatosensory Cortical Neurons Initiate Spike-and-Wave Discharges in a Genetic Model of Absence Seizures. *Journal of Neuroscience*, *27*(24), 6590–6599. https://doi.org/10.1523/JNEUROSCI.0753-07.2007

Puigcerver, A., van Luijtelaar, E. L. J. M., Drinkenburg, W. H. I. M., & Coenen, A. L. M. (1996). Effects of the GABAB antagonist CGP 35348 on sleep-wake states, behaviour, and spike-wave discharges in old rats. *Brain Research Bulletin*, *40*(3), 157–162. https://doi.org/10.1016/0361-9230(96)00046-9

Ratté, S., Hong, S., De Schutter, E., & Prescott, S. A. (2013). Impact of Neuronal Properties on Network Coding: Roles of Spike Initiation Dynamics and Robust Synchrony Transfer. *Neuron*, *78*(5), 758–772. https://doi.org/10.1016/j.neuron.2013.05.030

Rich, S., Booth, V., & Zochowski, M. (2016). Intrinsic Cellular Properties and Connectivity Density Determine Variable Clustering Patterns in Randomly Connected Inhibitory Neural Networks. *Frontiers in Neural Circuits*, *10*. https://doi.org/10.3389/fncir.2016.00082

Sanchez-Vives, M. V., Barbero-Castillo, A., Perez-Zabalza, M., & Reig, R. (2021). GABAB receptors: Modulation of thalamocortical dynamics and synaptic plasticity. *Neuroscience*, *456*, 131–142. https://doi.org/10.1016/j.neuroscience.2020.03.011

Slaght, S. J., Leresche, N., Deniau, J.-M., Crunelli, V., & Charpier, S. (2002). Activity of Thalamic Reticular Neurons during Spontaneous Genetically Determined Spike and Wave Discharges. *Journal of Neuroscience*, *22*(6), 2323–2334. https://doi.org/10.1523/JNEUROSCI.22-06-02323.2002

Sorokin, J. M., Davidson, T. J., Frechette, E., Abramian, A. M., Deisseroth, K., Huguenard, J. R., & Paz, J. T. (2017). Bidirectional Control of Generalized Epilepsy Networks via Rapid Real-Time Switching of Firing Mode. *Neuron*, *93*(1), 194–210. https://doi.org/10.1016/j.neuron.2016.11.026

Staak, R., & Pape, H.-C. (2001). Contribution of GABAA and GABAB Receptors to Thalamic Neuronal Activity during Spontaneous Absence Seizures in Rats. *Journal of Neuroscience*, *21*(4), 1378–1384. https://doi.org/10.1523/JNEUROSCI.21-04-01378.2001

Steriade, M. (2001). Impact of Network Activities on Neuronal Properties in Corticothalamic Systems. *Journal of Neurophysiology*, *86*(1), 1–39. https://doi.org/10.1152/jn.2001.86.1.1

Steriade, M., & Amzica, F. (1998). Slow sleep oscillation, rhythmic K-complexes, and their paroxysmal developments. *Journal of Sleep Research*, *7*(S1), 30–35. https://doi.org/10.1046/j.1365-2869.7.s1.4.x

Steriade, M., & Contreras, D. (1995). Relations between cortical and thalamic cellular events during transition from sleep patterns to paroxysmal activity. *Journal of Neuroscience*, *15*(1), 623–642. https://doi.org/10.1523/JNEUROSCI.15-01-00623.1995

Steriade, M., Deschenes, M., Domich, L., & Mulle, C. (1985). Abolition of spindle oscillations in thalamic neurons disconnected from nucleus reticularis thalami. *Journal of Neurophysiology*, *54*(6), 1473–1497. https://doi.org/10.1152/jn.1985.54.6.1473

Steriade, M., McCormick, D. A., & Sejnowski, T. J. (1993). Thalamocortical Oscillations in the Sleeping and Aroused Brain. *Science*, *262*(5134), 679–685.

Stiefel, K. M., & Ermentrout, G. B. (2016). Neurons as oscillators. *Journal of Neurophysiology*, *116*(6), 2950–2960. https://doi.org/10.1152/jn.00525.2015

Stiefel, K. M., Gutkin, B. S., & Sejnowski, T. J. (2008). Cholinergic Neuromodulation Changes Phase Response Curve Shape and Type in Cortical Pyramidal Neurons. *PLOS ONE*, *3*(12), e3947. https://doi.org/10.1371/journal.pone.0003947

Timofeev, I., Bazhenov, M., Seigneur, J., & Sejnowski, T. (2012). Neuronal Synchronization and Thalamocortical Rhythms in Sleep, Wake and Epilepsy. In J. L. Noebels, M. Avoli, M. A. Rogawski, R. W. Olsen, & A. V. Delgado-Escueta (Eds.), *Jasper's Basic Mechanisms of the Epilepsies* (4th ed.). National Center for Biotechnology Information (US). http://www.ncbi.nlm.nih.gov/books/NBK98144/

van de Bovenkamp-Janssen, M. C., van der Kloet, J. C., van Luijtelaar, G., & Roubos, E. W. (2006). NMDA-NR1 and AMPA-GluR4 receptor subunit immunoreactivities in the absence epileptic WAG/Rij rat. *Epilepsy Research*, *69*(2), 119–128. https://doi.org/10.1016/j.eplepsyres.2006.01.003

Vergnes, M., Marescaux, C., Depaulis, A., Micheletti, G., & Warter, J. M. (1987). Spontaneous spike and wave discharges in thalamus and cortex in a rat model of genetic petit mal-like seizures. *Experimental Neurology*, *96*(1), 127–136. https://doi.org/10.1016/0014-4886(87)90174-9

Wang, Z., & Wang, Q. (2017). Eliminating Absence Seizures through the Deep Brain Stimulation to Thalamus Reticular Nucleus. *Frontiers in Computational Neuroscience*, *11*. https://doi.org/10.3389/fncom.2017.00022

Woodman, M. M., & Canavier, C. C. (2011). Effects of conduction delays on the existence and stability of one to one phase locking between two pulse-coupled oscillators. *Journal of Computational Neuroscience*, *31*(2), 401–418. https://doi.org/10.1007/s10827-011-0315-2

Zavvari, F., Modarres Mousavi, S. M., Ejlali, M., Barfi, S., & Karimzadeh, F. (2020). Glutamate Signaling Pathway in Absence Epilepsy: Possible Role of Ionotropic AMPA Glutamate Receptor Type 1 Subunit. *Iranian Journal of Pharmaceutical Research*, *19*(4), 410–418. https://doi.org/10.22037/ijpr.2020.112638.13869

Tables

Table 1. Summary of values for receptor conductance strength that are meaningful for oscillations in the network. The optimal values as well as conductance ranges of the synaptic receptor conductance strength were based on previous study (Destexhe, 1998). Locations: presynaptic neuron → postsynaptic neuron. The synaptic receptor is located on the postsynaptic neuron.

Receptor	Location	Optimal Value (µS)	Conductance Range (µS)
AMPA	PY → PY	0.6	0.3 - 0.9
	PY → IN	0.2	0.06 - 2
	TC → RE	0.2	0 - 5
	TC → PY	1.2	0.15 - 5
	TC → IN	0.4	0 - 5
	PY → RE	1.2	0.4 - 5
	PY → TC	0.01	0 - 0.1
GABA$_A$	RE → RE	0.2	0 - 1.2
	RE → TC	0.02	0 - 1
GABA$_B$	IN → PY	0.03	0.02 - 5
	RE → TC	0.04	0.01 - 5

Table 2. Summary of parameters tested in the Knox model. Only values for the conductance of AMPA receptors located on RENs that receives excitatory input from PYNs are included, as optimal values of other conductance strengths were used and kept constant in this model. The bolded values indicate that the conductance strength is increased from the optimal value; italicized and underlined values indicate that the receptor conductance strength is decreased from the optimal value. Synapse type: PYRE = excitatory projection from PYNs to AMPA receptors located on RENs.

Trial #	21	22	23	24	25
PYRE	1.2	_1.0_	**1.8**	**2.4**	**3.6**

Table 3. Summary of parameters tested in the RE-TC-PY network. The conductance values of intra-RE synapses, RE-TC synapses, intra PY synapses, PY-TC synapses mediated by AMPA receptors, PY-IN synapses mediated by AMPA receptors, as well as IN-PY synapses mediated by GABA$_B$ receptors were not shown, as the optimal values were used for each type of synapses. The bolded values indicate that the conductance strength is increased from the optimal value; italicized and underlined values indicate that the conductance strength is decreased from the optimal value. Synapse types: INPYa = inhibitory projection from IN to GABA$_A$ receptors located on PY neurons; TCPY = excitatory projection from TC to AMPA receptors located on PY neurons.

Trial #	INPYa (µS)	TCPY (µS)
16	0.15*50%	1.2
17	0.15*50%	_0.6_
18	0.15*50%	**2.4**
19	0.15*100%	1.2
20	0.15*100%	**2.4**

Table 4. Summary of parameters for receptor conductance strength tested in the decorticated RE-TC thalamic network. Conductance values for intra-cortical connections were irrelevant in this reduced model, so they were not shown. The bolded values indicate that the conductance strength is increased from the optimal value; italicized and underlined values indicate that the receptor conductance strength is decreased from the optimal value. Synapse types: RERE = intra RE synapses mediated by GABA$_A$ receptors; RETCa = inhibitory projection from TCNs to GABA$_A$ receptors located on RENs; RETCa = inhibitory projection from TCNs to GABA$_B$ receptors located on RENs; TCRE = excitatory projection from TCNs to AMPA receptors located on RENs.

Trial #	RERE (µS)	RETCa (µS)	RETCb (µS)	TCRE (µS)
1	0.2	0.02	0.04	0.2
2	_0.1_	0.02	0.04	0.2
3	_0.1_	_0.01_	0.04	0.2
4	**0.4**	**0.04**	0.04	0.2
5	0.2	0.02	**0.08**	0.2
6	0.2	0.02	_0.02_	0.2
7	0.2	0.02	**0.16**	0.2
8	0.2	0.02	**0.20**	0.2
9	**0.4**	0.02	**0.24**	0.2
10	0.2	0.02	0.04	_0.1_
11	0.2	0.02	0.04	**0.4**
12	0.2	0.02	0.04	**0.6**
13	0.2	0.02	0.04	**1.2**
14	0.2	0.02	0.04	**2**
15	0.2	0.02	0.04	**4**

Figures

Figure 1. Schematic diagram for the thalamocortical network. The red directional arrows represent excitatory synapses (TC→RE, TC→IN, TC→PY, PY→PY, PY→IN, PY→RE, PY→TC) mediated by AMPA receptors. Blue directional arrows represent inhibitory synapses (RE→TC, IN→PY) mediated by a mixture of $GABA_A$ and $GABA_B$ and receptors. Green arrow represents the intra-RE synapses mediated by $GABA_A$ receptors. The simplified version of this model is shown in the purple circle, containing only the thalamic neurons.
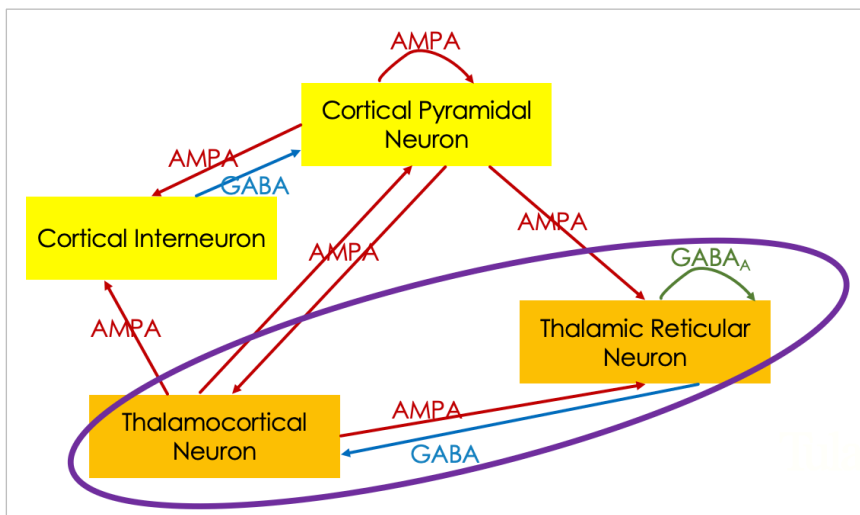
Figure 2. Collective activities of all PYNs, RENs, and TCNs during simulation in the Knox model. Each panel corresponds to the collective firing activities of a specific type of neurons over time in this model. Specifically, A) shows an 8-10 Hz spindle oscillation with two clusters of TCNs with alternating firing activities, as well as two clusters of RENs with alternating bursts; B) shows a 3-4 Hz SW oscillations with synchronized activities in TCNs and RENs. The y-axis in each panel represents the indexes of neurons (1 to 100), and the x-axis displays the time. The color corresponds to the voltage of the cell, with darker blue representing a more hyperpolarized state and darker red representing a more depolarized state. Hence, the brighter bands in each panel represent the collective firing of action potentials. Adapted from Knox et al., 2018 Figure 2.
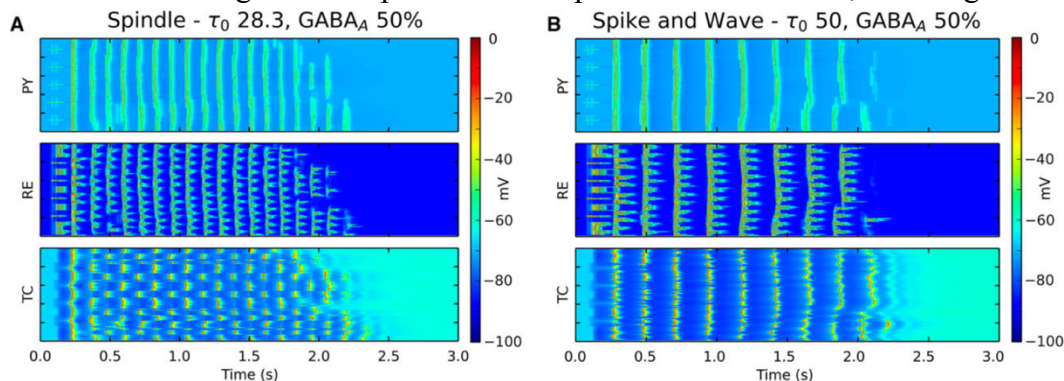
Figure 3. Comparison of network architectures. The green directional arrows represent excitatory AMPA synapses from TC neurons to RE neurons. Blue directional arrows represent intra RE inhibitory synapses mediated by GABA$_A$ receptors. Dashed directional arrows are the connections that were rewired from the chain architecture to the ring architecture. Specifically, A) shows the chain architecture of the network connectivity in the original Knox model, where neurons towards both ends connect to neighboring neurons twice; B) shows the re-wired ring architecture of the connectivity where none of the synaptic connection would be repeated. Only synaptic projections of the second neuron of each type were shown as a conceptual demonstration.

A) Original model.
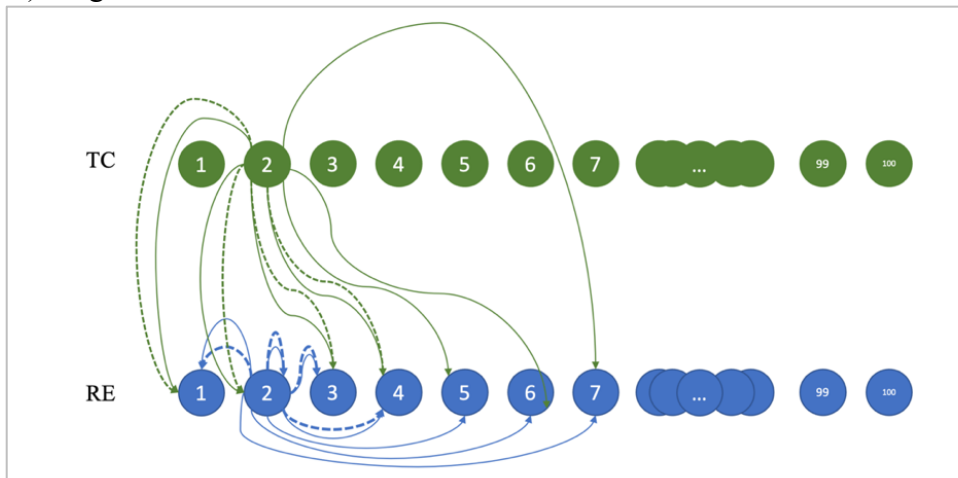
B) Ring model.
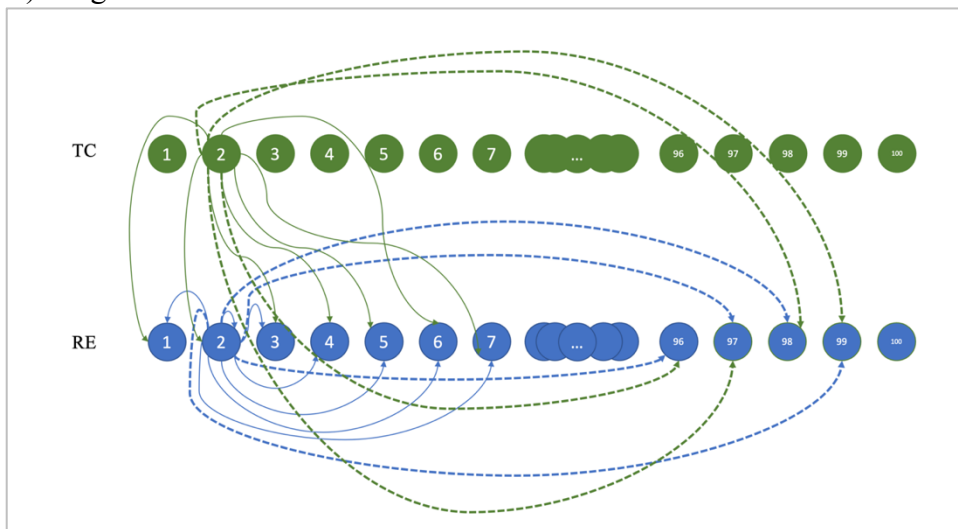
Figure 4. Effects of changing PY→RE AMPA receptor conductance in the Knox model.
A) Trial 21. Control figure. Parameters used here were the same as the parameters for generating spindle oscillation.

B) Trial 22. Reducing the PY→RE AMPA receptor conductance to 50% of the optimal conductance value.
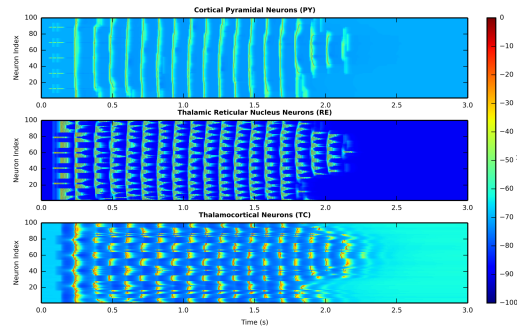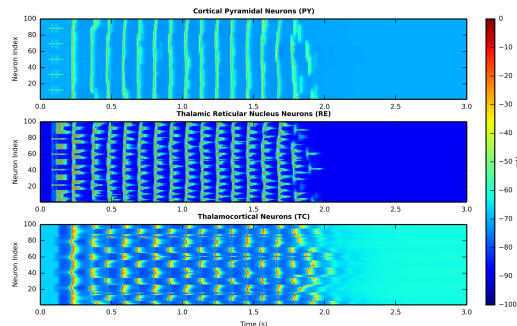
C) Trial 23. Increasing PY→RE AMPA receptor conductance to 150% of the optimal conductance value.
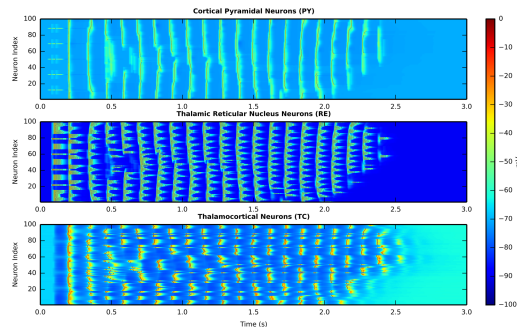
D) Trial 24. Increasing PY→RE AMPA receptor conductance to 200% of the optimal conductance value.
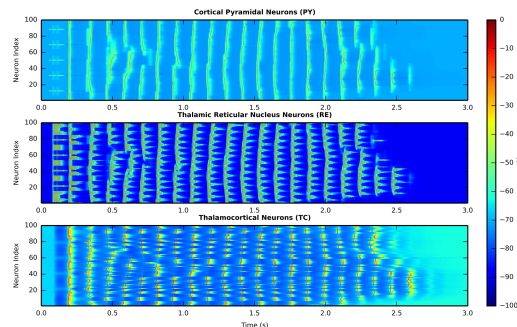
Figure 5. Raster plots for TCNs and RENs in the Knox model with a chain architecture.
A) Spindle oscillations raster plots of TCNs and RENs in the Knox model.
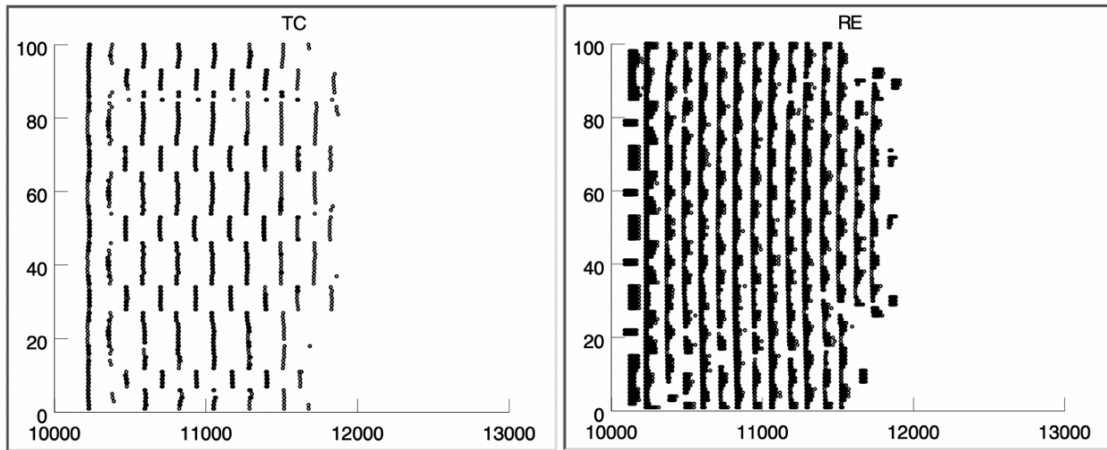
B) SW oscillations raster plots of TCNs and RENs in the Knox model.
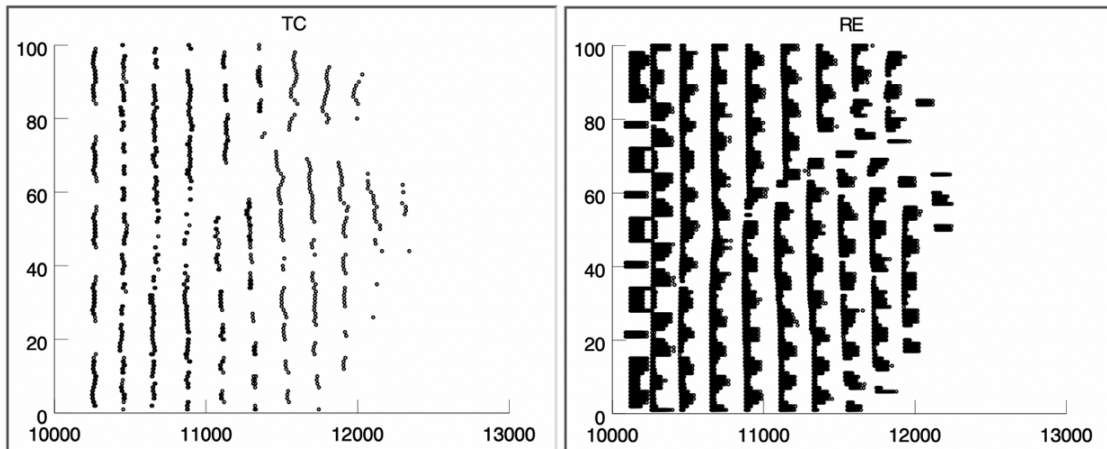
Figure 6. Raster plots for TCNs and RENs in the Knox model with a ring architecture.
A) Spindle oscillations raster plots of TCNs and RENs in the Knox model with ring
architecture.
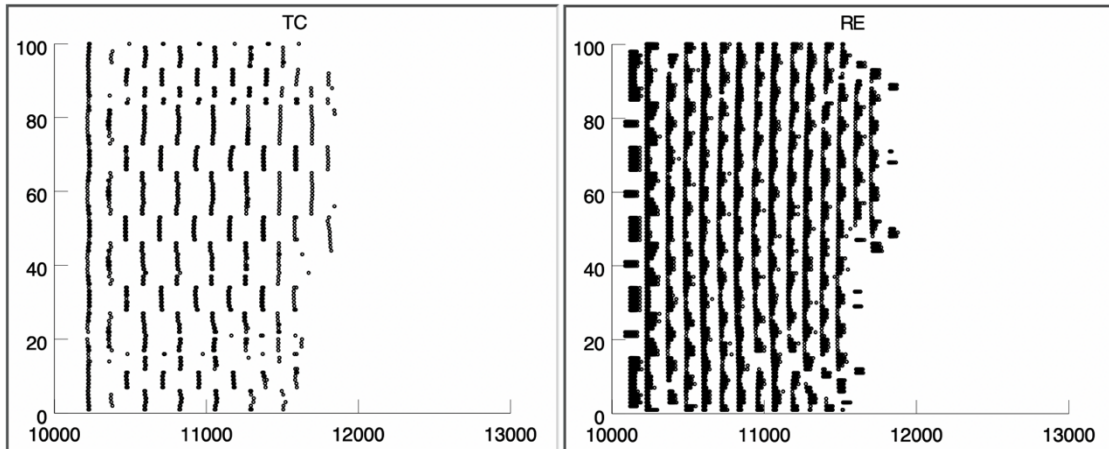
B) SW oscillations raster plots of TCNs and RENs in the Knox model with ring
architecture.
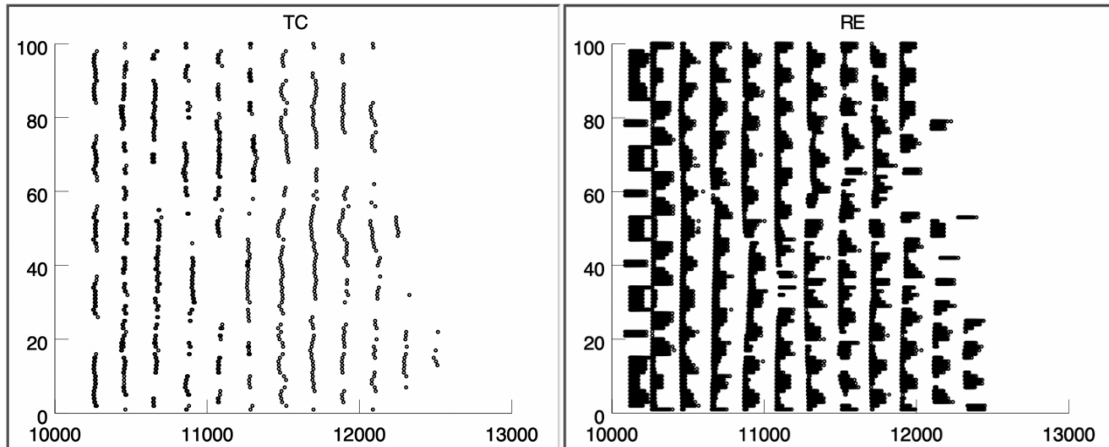
Figure 7. Effects of conductance changes in the reduced model with chain architecture.
A) Schematic diagram of the reduced model.

B) Trial 19. Control with previously determined optimal synaptic conductance.
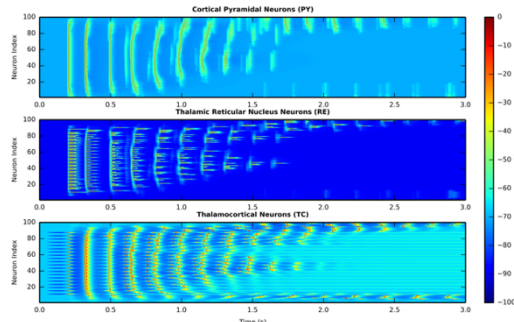
C) Trial 16. Reducing IN→PY GABA$_B$ receptor conductance to 50% of the optimal conductance value.
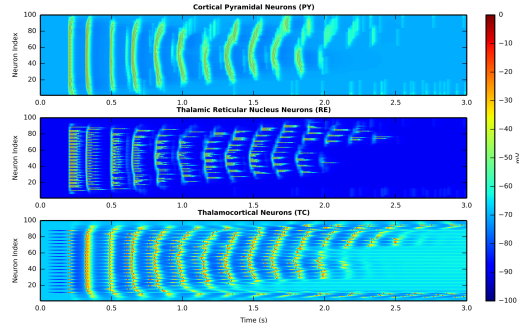
D) Trial 20. Increasing TC→PY AMPA receptor conductance to 200% of the optimal conductance value.
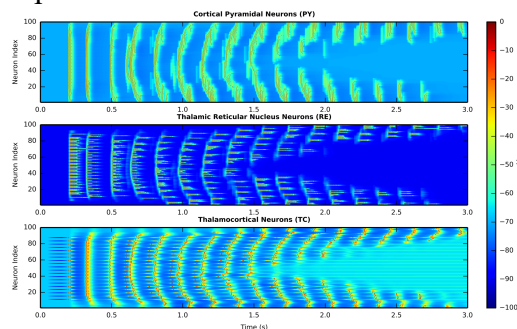
E) Trial 17. Reducing TC→PY AMPA receptor conductance to 50% of the optimal value with 50% of optimal IN→PY GABA$_A$ receptor conductance.
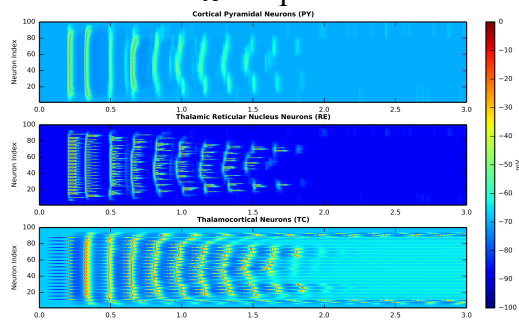
F) Trial 18. Increasing TC→PY AMPA receptor conductance to 200% of optimal value with 50% of optimal IN→PY GABA$_A$ receptor conductance.
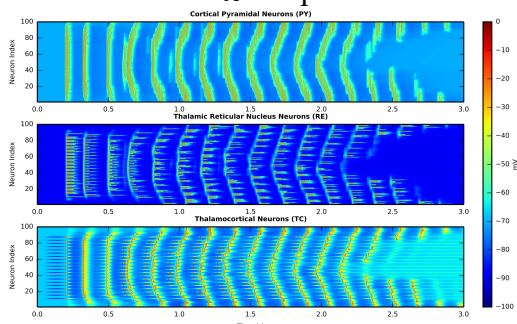
Figure 8. Effects of changing the conductance of intra-RE GABA$_A$ receptor, RE→TC GABA$_A$ receptor, RE→TC GABA$_B$ receptor, and AMPA receptor in the decorticated model.

A) Schematic diagram of the decorticated model.

B) Trial 1. Control with optimal receptor conductance.
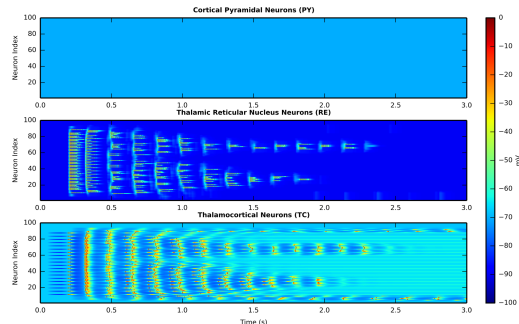
C) Trial 2. Decreasing the intra-RE GABA$_A$ receptor conductance to 50% of optimal value.
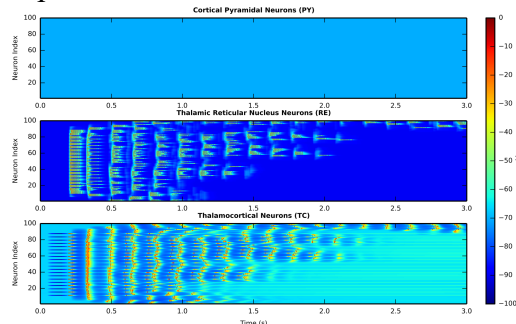
D) Trial 9. Increasing the intra-RE GABA$_A$ and RE→TC GABA$_B$ receptor conductance to 200% of optimal values.
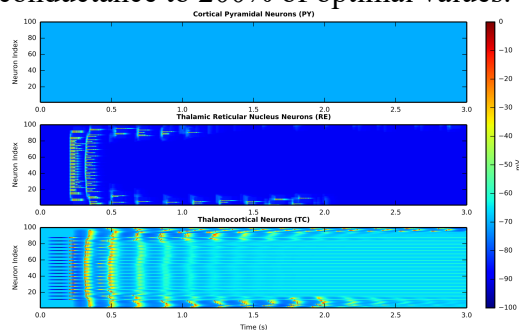
E) Trial 3. Reducing both intra-RE and RE→TC GABA$_A$ conductance to 50% of optimal values.
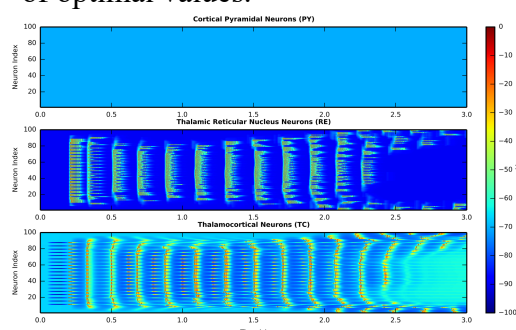
F) Raster plot for TCNs in trial 3.
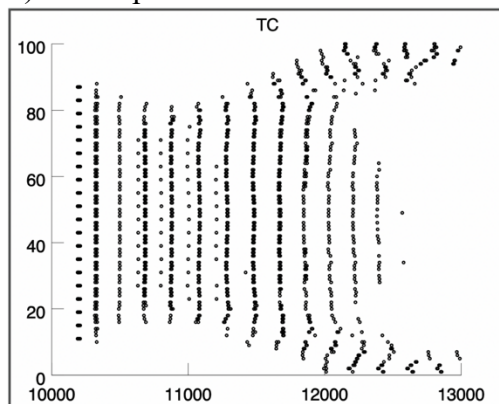
G) Trial 4. Increasing both intra-RE and RE→TC GABA$_A$ conductance to 200% of optimal values
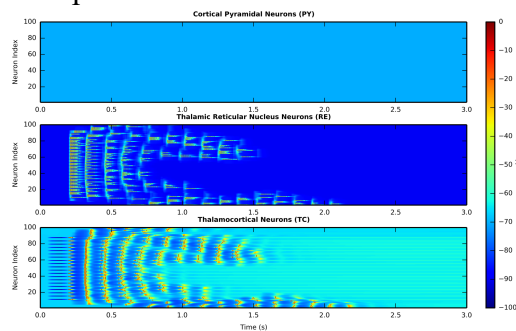
Figure 9. Effects of changing RE→TC GABA_B receptor conductance in the decorticated model.

A) Trial 6. Reducing RE→TC GABA_B receptor conductance to 50% of optimal value.
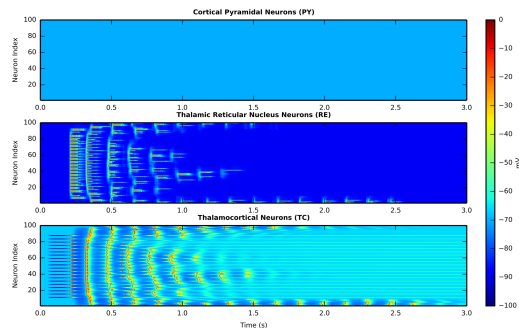
B) Trial 5. Increasing RE→TC GABA_B receptor conductance to 200% of optimal value.
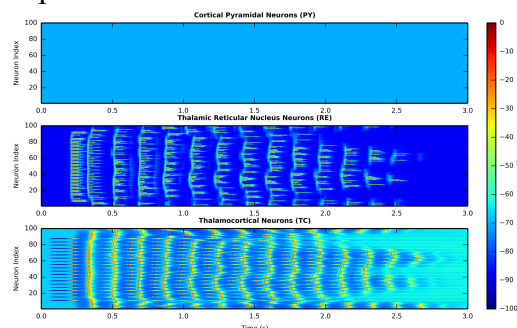
Figure 10. Effects of changing TC→RE AMPA receptor conductance in the decorticated model.

A) Trial 10. Reducing TC→RE AMPA receptor conductance to 50% of optimal value.
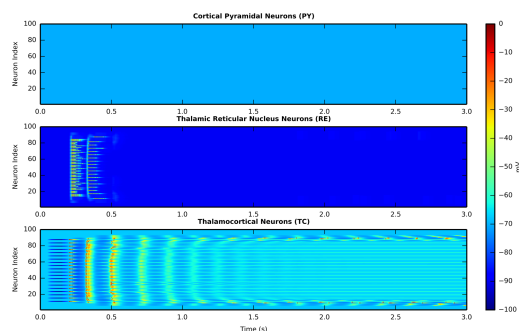
B) Trial 11. Increasing TC→RE AMPA receptor conductance to 200% of optimal value.
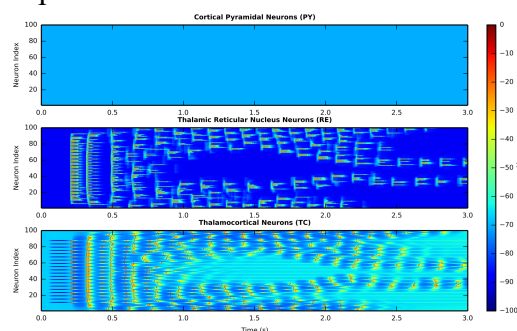
C) Trial 12. Increasing TC→RE AMPA receptor conductance to 300% of optimal value.
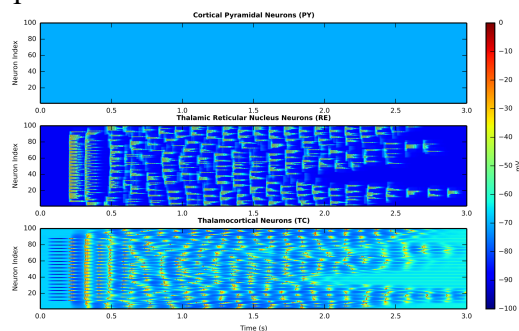
D) Trial 13. Increasing TC→RE AMPA receptor conductance to 600% of optimal value.
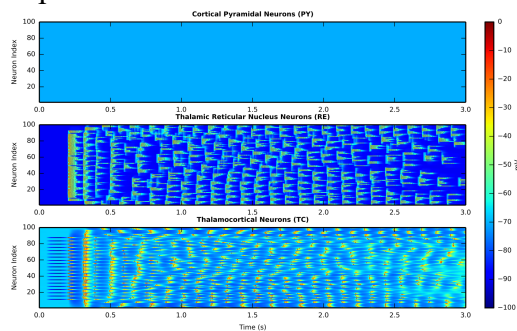
Figure 11. Stimulus applied throughout the simulation in the decorticated model.
A) Raster plots of TCNs and RENs under optimal receptor conductance for spindle oscillations.
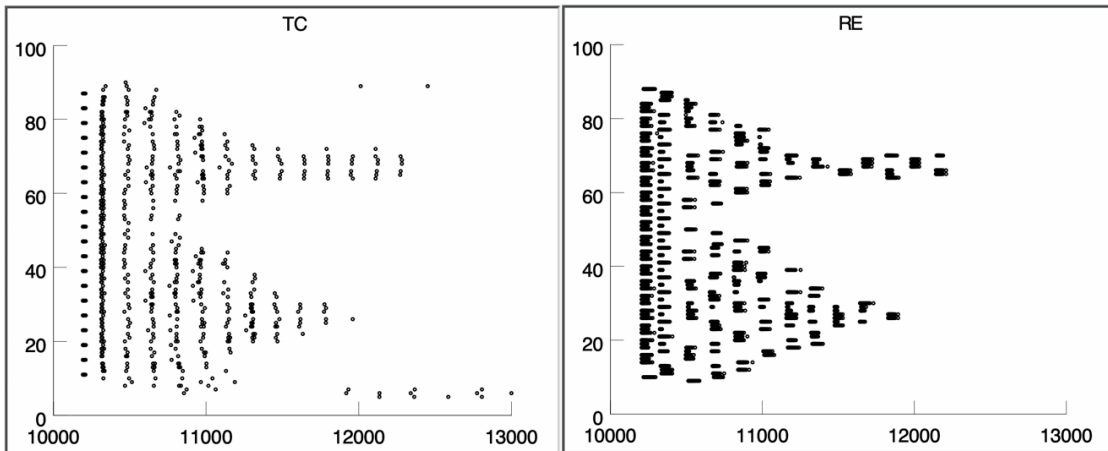
B) Sustained firing activities of TCNs and RENs under optimal receptor conductance for spindle oscillations with prolonged stimulus.
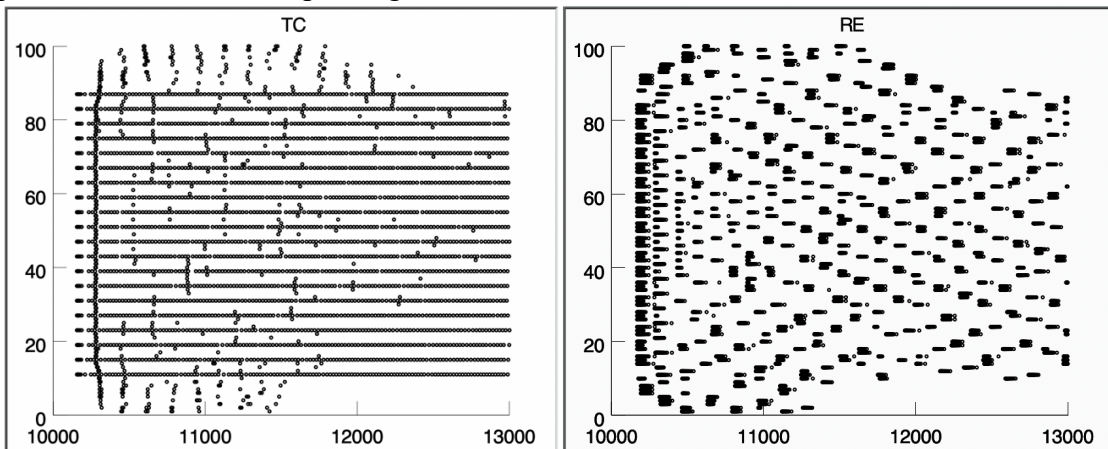
Figure 12. Constant stimulus applied on all RENs.
A) RENs in the chain architecture of the RE-TC circuit.
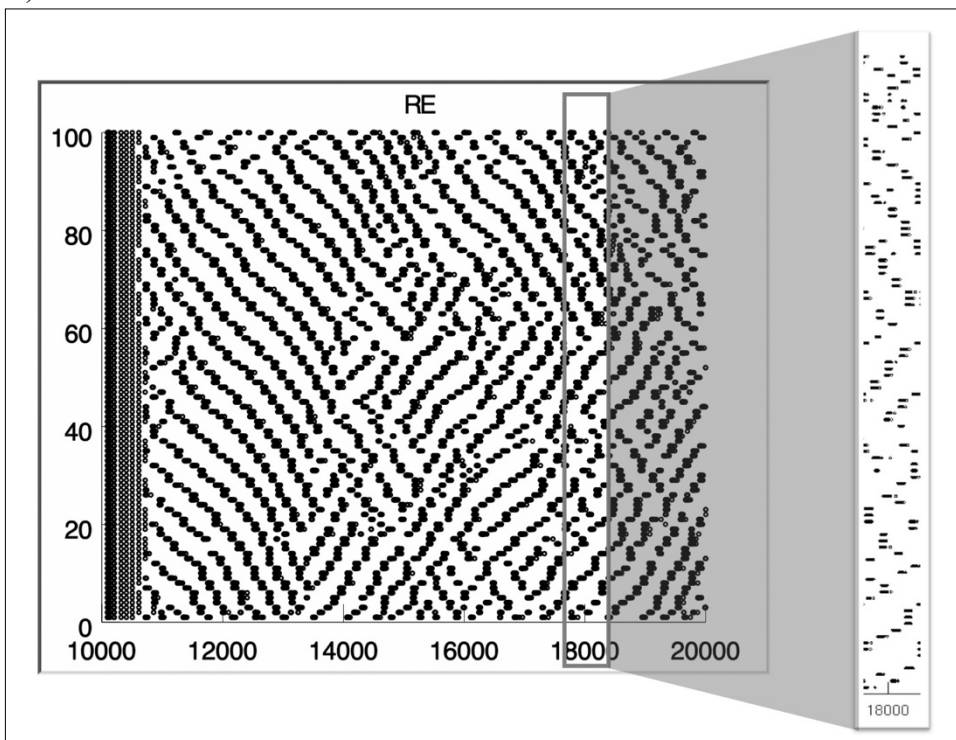
B) RENs in the ring architecture of the RE-TC circuit.
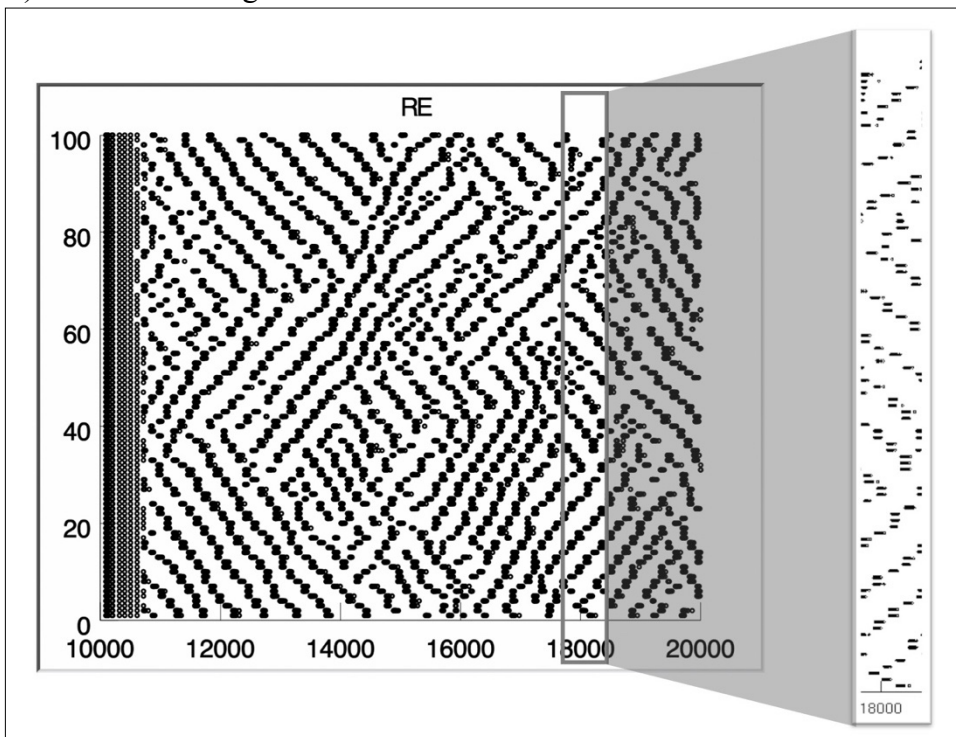
Figure 13. Traveling wave and burst duration in RENs.
A) Raster plot for RENs with optimal receptor conductance values and a depolarizing stimulus of 0.3 µA. $\tau_0 = 40$.
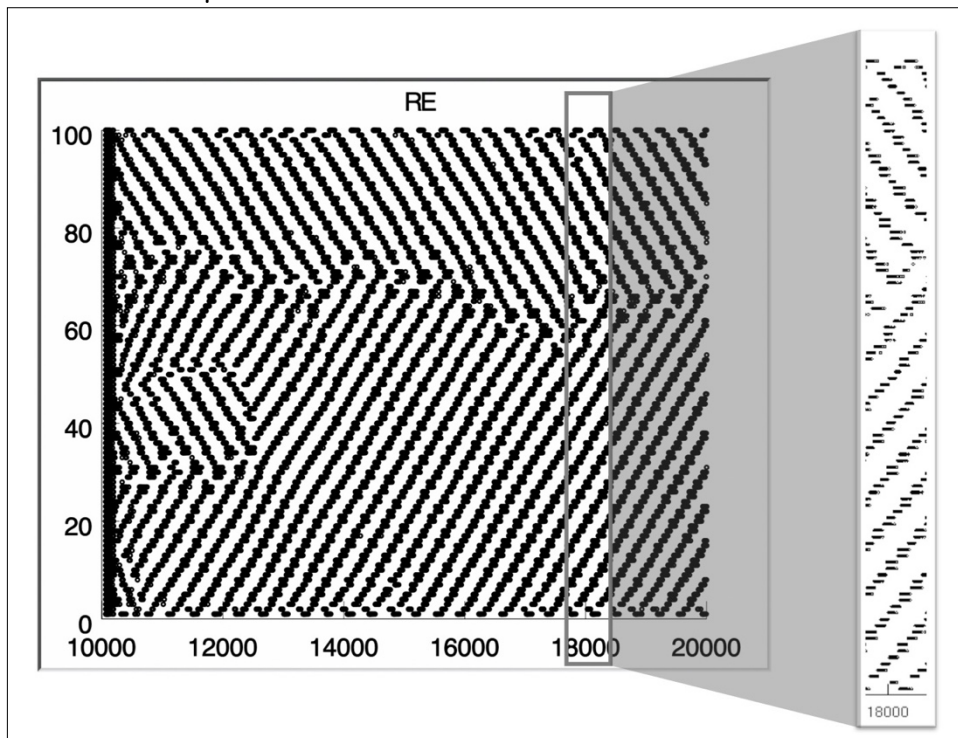
B) Raster plot for RENs with optimal receptor conductance values and a depolarizing stimulus of 0.3 µA. $\tau_0 = 50$.
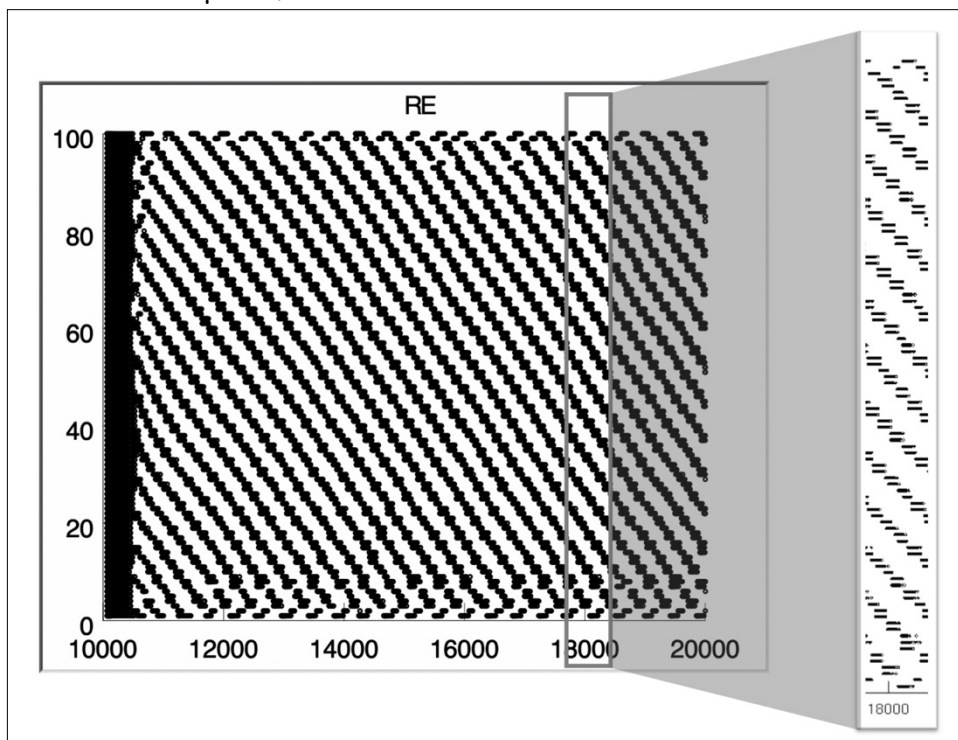
Figure 14. Single REN model under SWD parameter.
A) Voltage trace of this single REN in the model under SWD parameter.
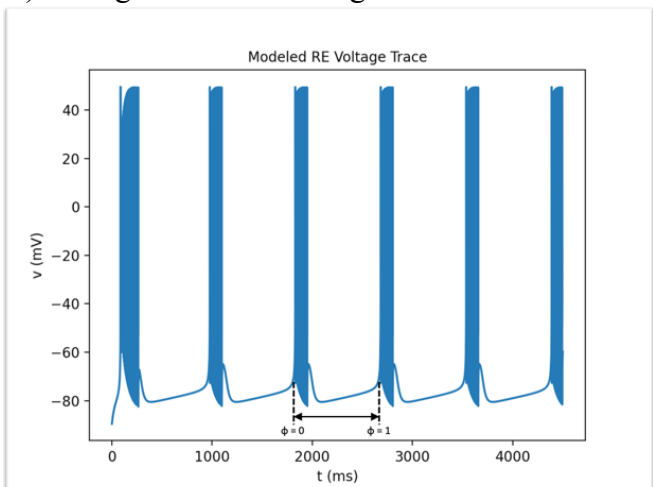
B) Voltage trace of REN with the index number 40 in the Knox model.
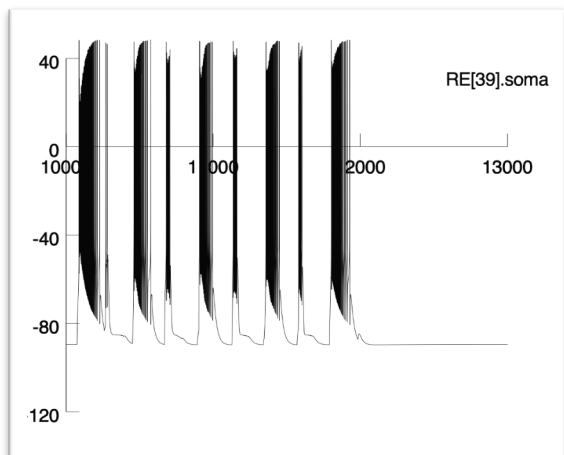
C) Depolarization-driven PRC for REN. Perturbations used are small current pulses of 0.06 µA.
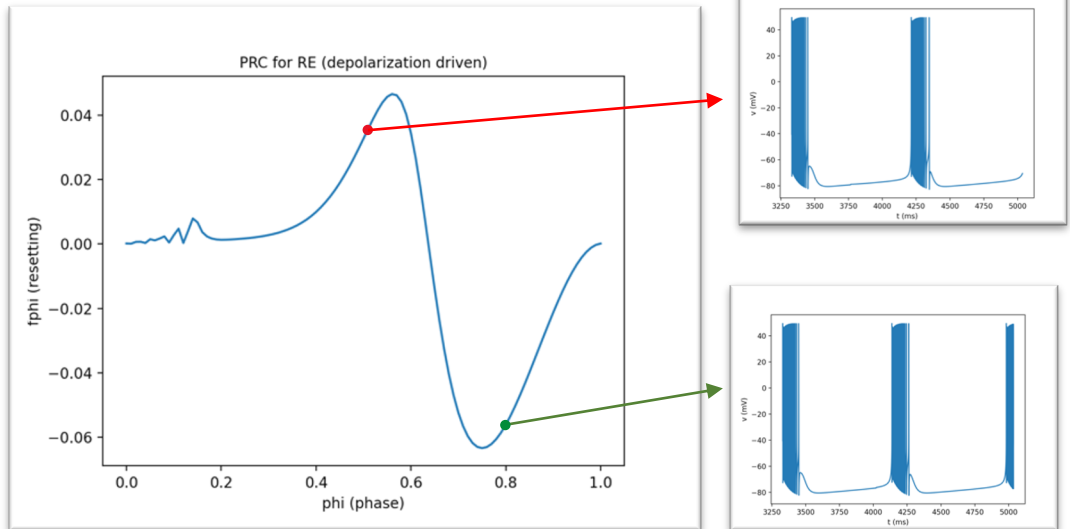
D) Conductance-driven-perturbations PRC for REN. Perturbations used are based on intra-RE GABA$_A$ receptor conductance.
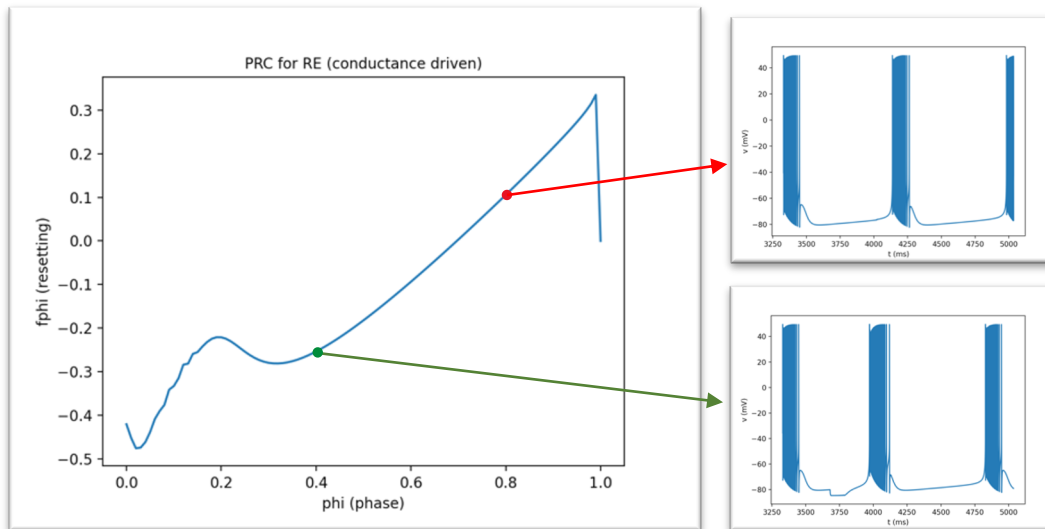
Figure 15. Single REN model under spindle parameter.
A) Voltage trace of this single REN in the model under spindle parameter.
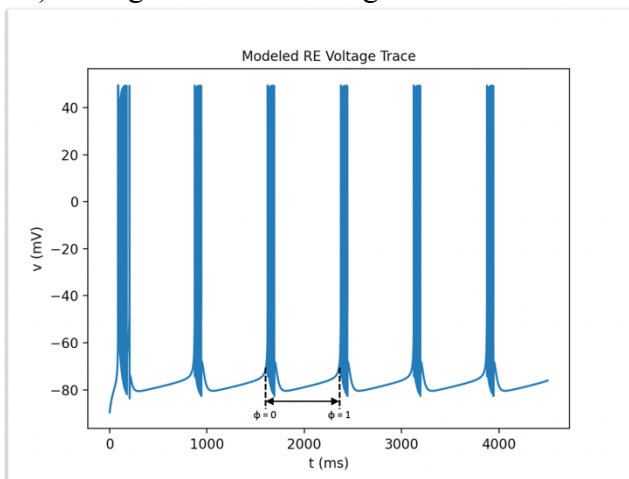
B) Voltage trace of REN with the index number 40 in the Knox model.
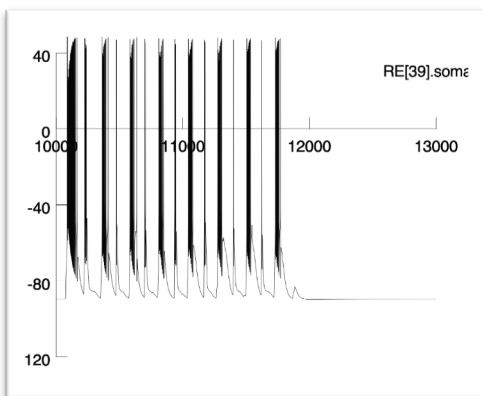
C) Depolarization-driven PRC for REN. Perturbations used are small current pulses of 0.06 μA.
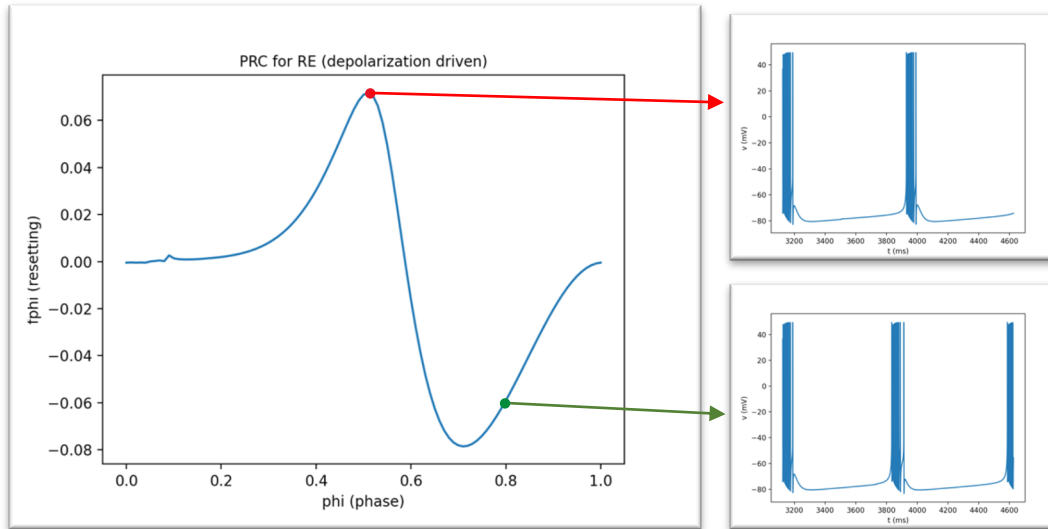
D) Conductance-driven PRC for REN. Perturbations used are based on intra-RE GABA$_A$ receptor conductance.
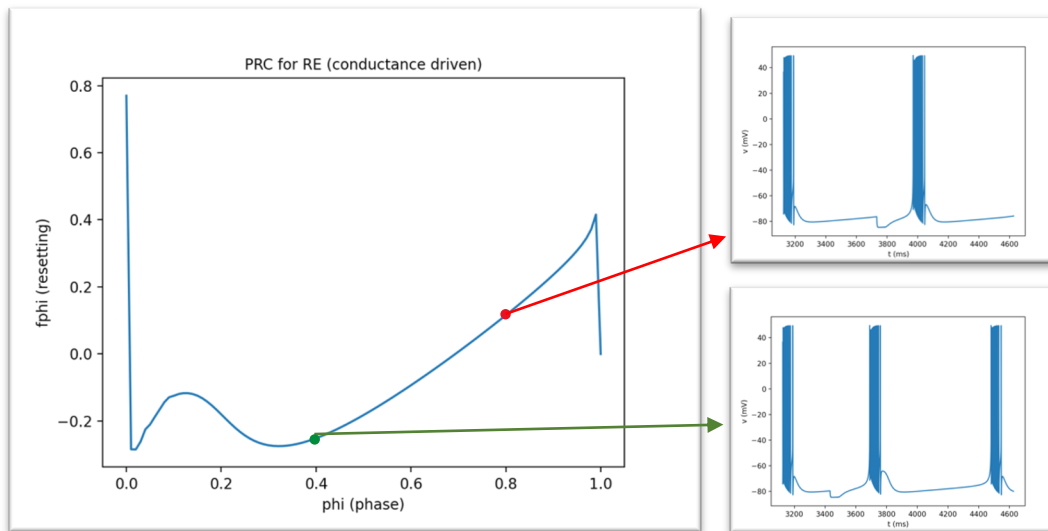
Figure 16. Reciprocally connected RE-TC model under SWD parameter.

C) Voltage trace of TCN with the index number 40 in the Knox model.

E) PRC for RE (intraRE GABAa conductance)

F) PRC for RE (TCRE AMPA conductance)

G) PRC for TC (RETC GABA driven)
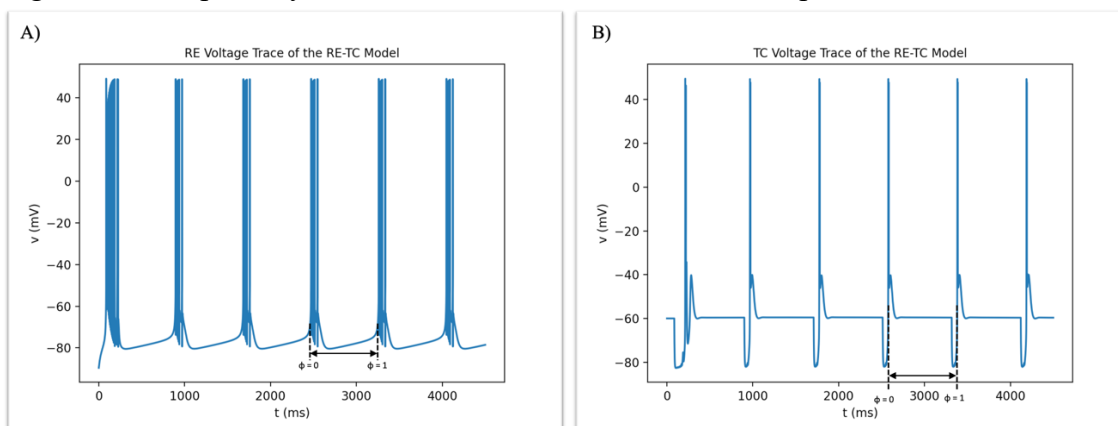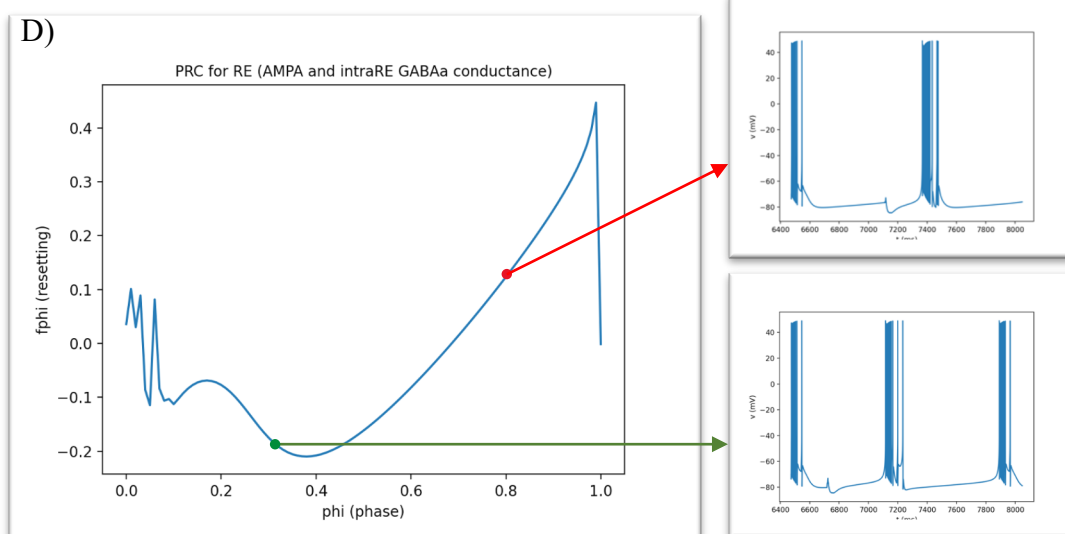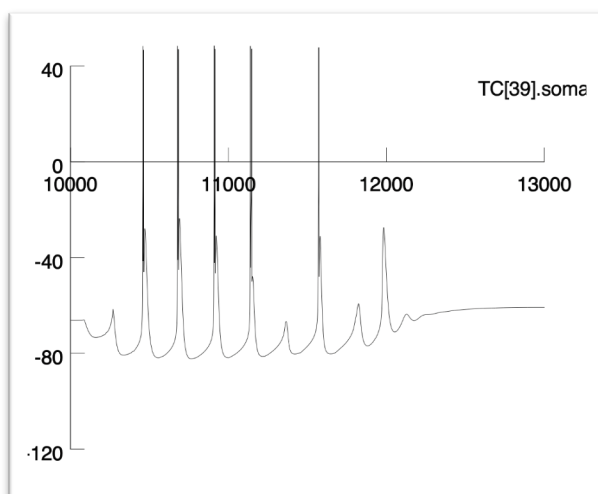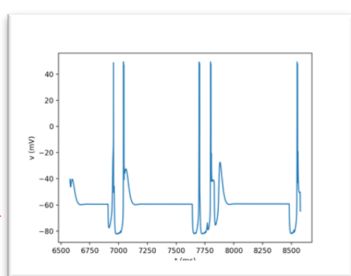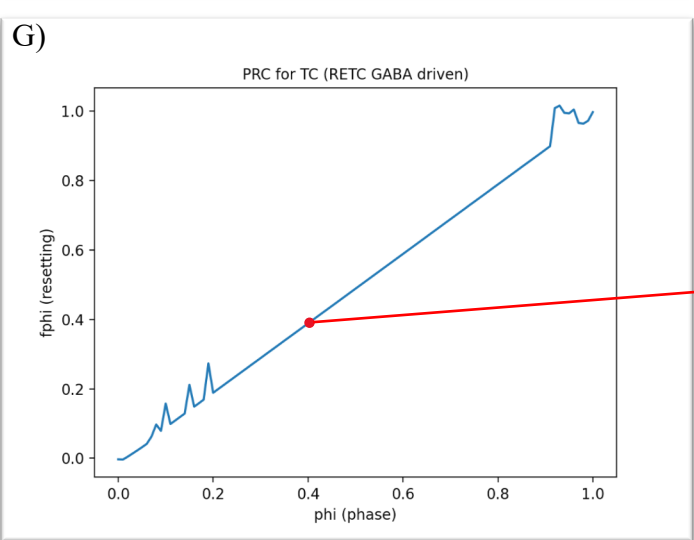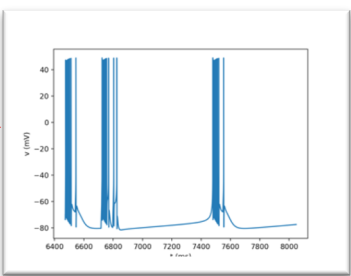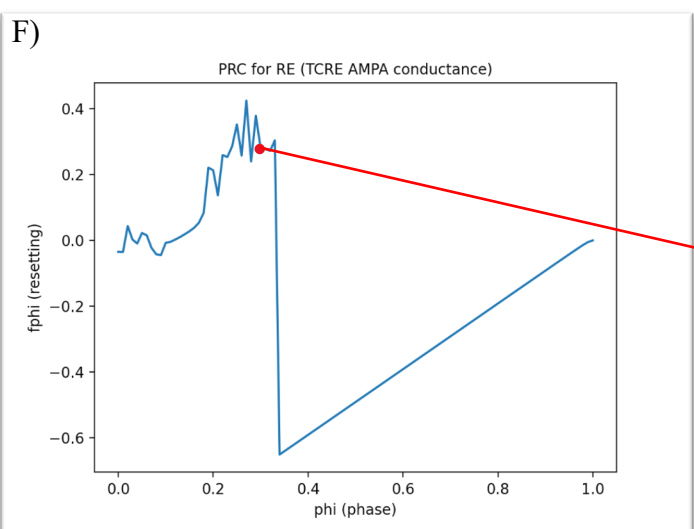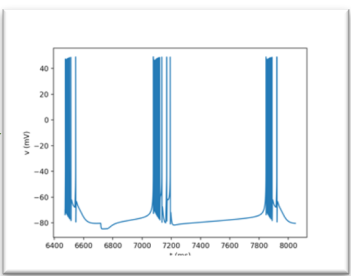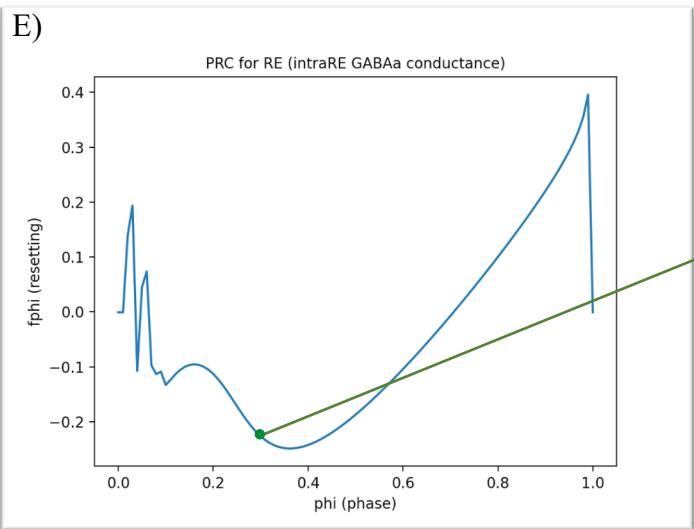
Figure 17. Reciprocally connected RE-TC model under spindle parameter.

C) Voltage trace of TCN with the index number 40 in the Knox model.

E)

F)

G)
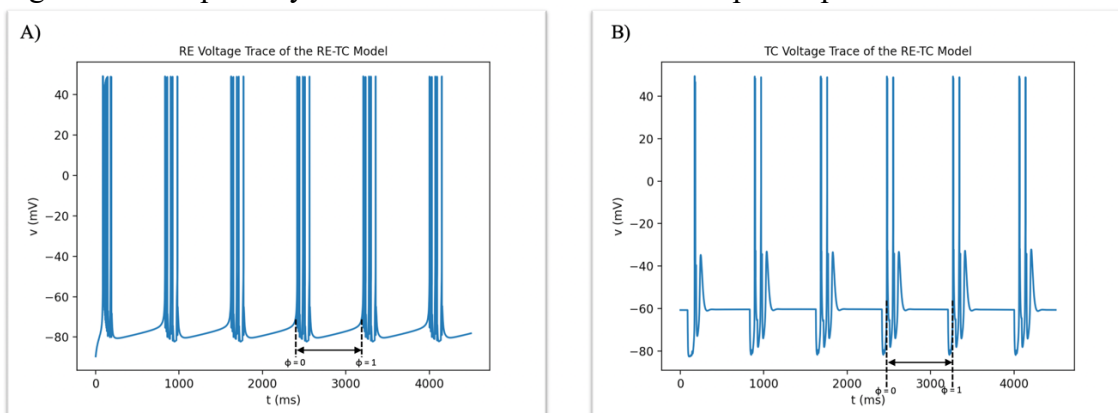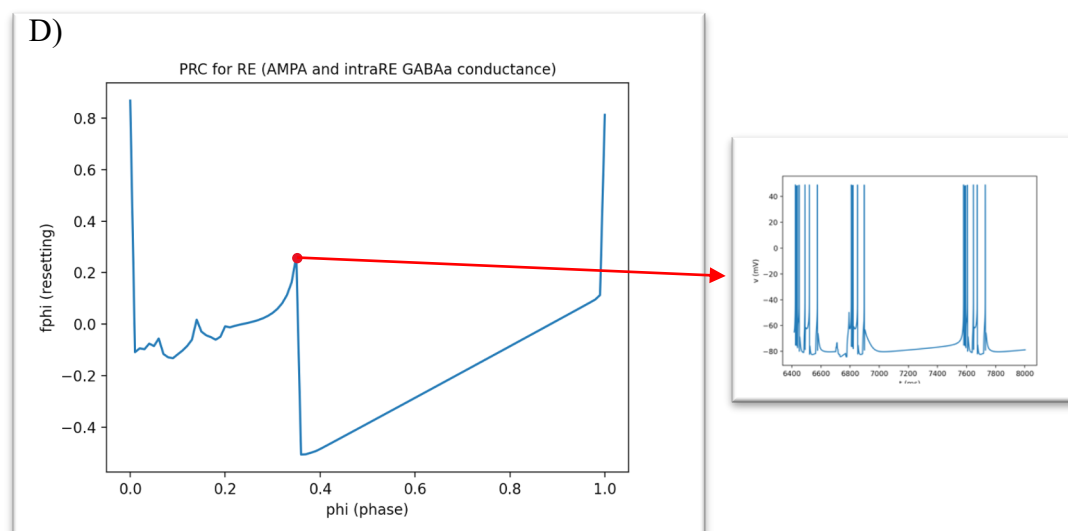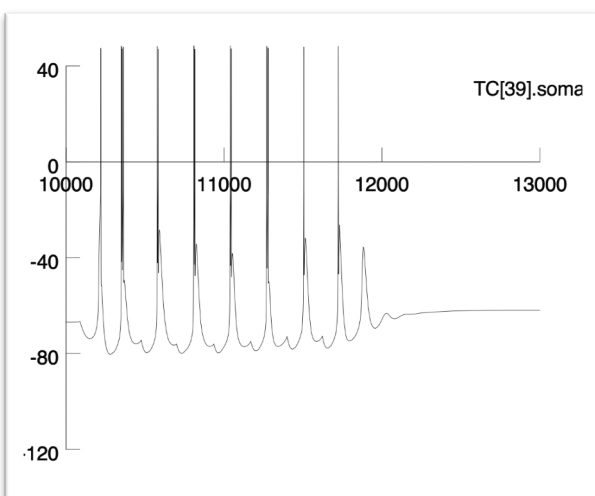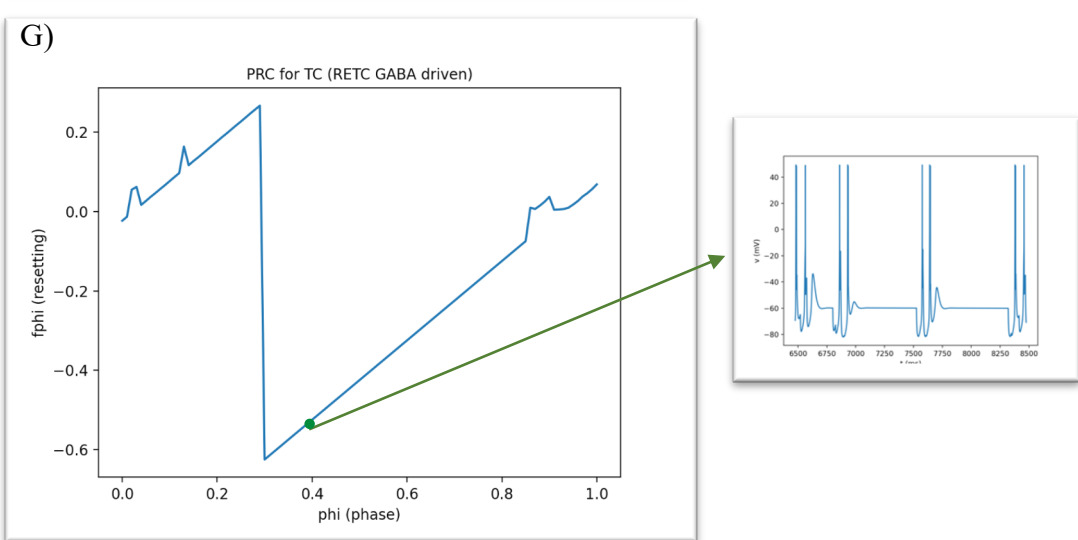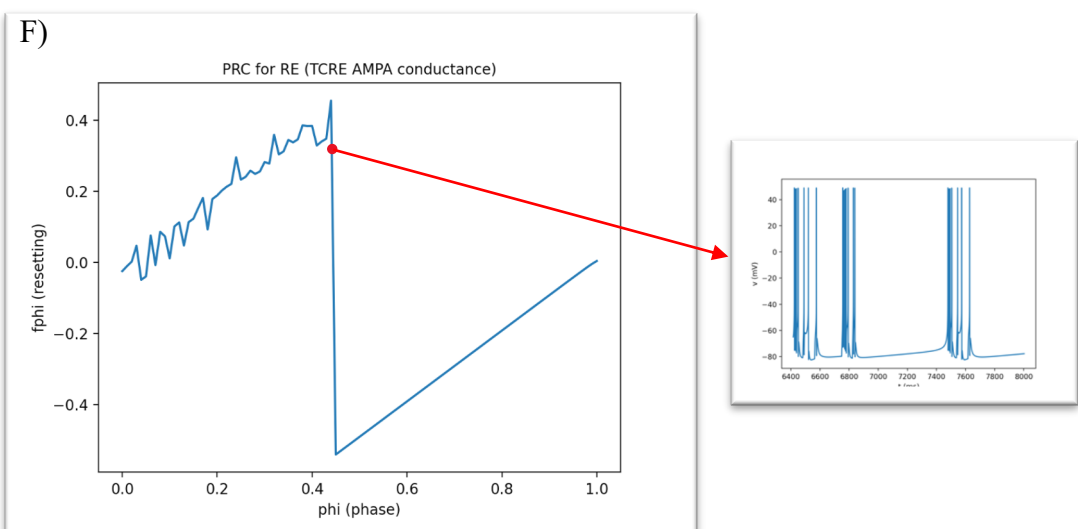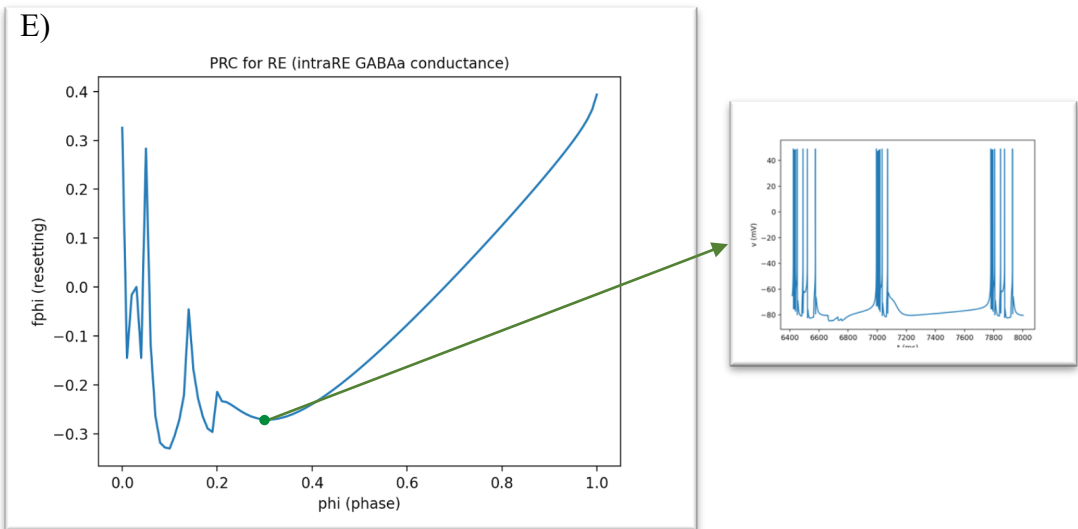
Biography

Hanyun Wang received her Bachelor of Science in Neuroscience and Bachelor of Arts in Economics from Tulane University in 2020. In the Spring 2020 semester, she assisted with the computational aspect of the Shox2 project in Dr. Laura Schrader's lab. She then joined the 4+1 Master's in Neuroscience program in Fall 2020 where she continued her research in the thalamocortical circuit using the computational model that was originally developed by Destexhe. After receiving her Master's degree, she is planning on working in a lab as a research technician for a while before applying for a doctoral program in neuroscience.